TÉCNICO LISBOA

Seismic Inversion of under-sampled reservoirs

Astrid de Jesus Torres Fernandez

Thesis to obtain the Master of Science Degree in

Petroleum Engineering

Supervisors: Prof. Amilcar de Oliveira Soares
Msc. Dario Sergio Cersosimo

Examination Committee

Chairperson: Prof. Maria Joao Correia Colunas Pereira
Supervisor: Prof. Amilcar de Oliveira Soares
Member of the Committee: PhD. Miles Leggett

October 2015

Abstract

In this project are performed two different approaches of seismic inversion: a deterministic, given by a model-based inversion and a stochastic executed following a global stochastic inversion methodology. The wavelet to be used in both approaches is extracted from the seismic, considering a statistical method. Two pseudo- logs of acoustics impedance were generated: i) by extraction of a trace from the interval velocity section and using Gardner's relationship to calculate the density and then performing the calculations of the acoustic impedance. ii) by extraction of a trace from the result of the deterministic inversion.

The Global Stochastic Inversion was executed considering three cases:

1. Using the second pseudo-log and as low frequency model one generated by the interpolation of the first pseudo-log and taking into consideration the geological information.
2. Using a model of geological zones and conditioning the GSI to the local acoustic impedance distributions taken from the second pseudo-log.
3. Using as input the output from the deterministic inversion and performing the simulations and co-simulations with direct sequential simulation with locally variable mean.

The results show that the technique allows to explore different scenarios regarding the spatial distribution of acoustic impedances and assessing the corresponding uncertainty of them. Another important issue observed in the results is about the quality of seismic data: in zones where this doubtful the variability of final acoustic impedances images is high, being poorly matched at the end of the inversion process and do not reproducing the noise in the final result.

Keywords: seismic inversion, acoustic impedance, deterministic inversion, stochastic inversion, model-based inversion, global stochastic inversion.

Resumo

Neste projeto são considerados duas metodologias de inversão sísmica, uma determinística realizada "Model Based Inversion" e uma metodologia estocástica de inversão geoestatística com um método de perturbação global. A "wavelet" utilizada em ambas metodologias foi extraída da sísmica utilizando um método estatístico. Foram gerados dois pseudo-poços de impedância acústica: i) extraindo um traço da secção de velocidade intervalar e utilizando a equação de Gardner para calcular a densidade e posteriormente a impedância acústica ii) extraindo um traço do cubo obtido da inversão determinística.

A inversão estocástica foi realizada considerando três casos:

1. Utilizando o segundo pseudo-poço como dado de entrada e um modelo gerado da interpolação do primeiro pseudo-poço, considerando a informação geológica, como modelo de baixa frequência.
2. Utilizando um modelo de zonas geológicas e condicionando a inversão a distribuições locais extraídas de um segundo pseudo-poço.
3. Usando como dado de entrada o resultado da inversão determinística e realizando as simulações e co-simulações com médias locais.

Os resultados mostram que a técnica proposta permite explorar diferentes cenários de distribuição espacial com a sua respetiva avaliação da incerteza. Outro aspeto importante é referente à qualidade dos dados sísmicos: em zonas onde a qualidade da sísmica é duvidosa a variabilidade das imagens finais obtidas para a impedância acústica é alta, permanecendo mal estimada no final do processo de inversão e não reproduzindo nos resultados finais o ruído presente nos dados sísmicos.

Palavras-chave: inversão sísmica, impedância acústica, inversão determinística, inversão estocástica, "Model based Inversion", inversão estocástica com um método de perturbação global.

ACKNOWLEDGEMENT

First of all, thanks to Professor Amilcar Soares for all the support, consideration and help in this two years. Thanks to all the staff in IST-CERENA, in special to Ruben Nunes for helping me with this project.

Thanks to the all the staff of Galp Exploration, in special to Elsa Azevedo e Silva and Miles Leggett for giving me the opportunity to develop this project in the company and for supporting me. Thanks to Sergio Cersosimo for being my advisor and for helping me during this process.

Thanks to my husband for supporting me in this goal and for encouraging me to take the decision to start this Master. Thanks to all my family and friends, that even in the distant they have been taking care of me in the past two years and cheering me up to achieve my goals.

Finally, thanks to all my colleagues from the Master for make me feel welcome.

CONTENTS

INDEX OF FIGURES

INDEX OF TABLES

LIST OF ABBREVIATIONS AND ACRONYMS

2D: Two dimensions

AI: Acoustic impedance

CERENA: Center of natural resources and environment

CDP: Common depth point

GSI: Global Stochastic Simulation

LFAF: Low frequency array filtering

ms: Milliseconds

PDF: Probabilistic Distribution Function

RMS: Root mean square

Vp: P-wave velocity

WEMA: Wave equation multiple attenuation

1. INTRODUCTION

The Seismic reflection method represents one of most important tools in hydrocarbon exploration, because it has a great power of resolution and penetration. In this method, a seismic artificial stimulus, given by a seismic wave, is induced into the subsurface and then the travel time of the wavelet from its generation until its reception is measured using recording equipment placed on the surface. Therefore with the travel times and estimation of the velocity of propagation it is possible to do a reconstruction of the trajectories of seismic waves. The travel time depends on factors such as the physical properties of the rocks, the structural geology of the area and the fluid content.

In Geophysics the direct problem is known as forward or simulation problem, which according to Tarantola (2005), is defined as the prediction of the outcomes of measurements, given a complete description of a physical system. The forward modeling for seismic inversion is based in the convolutional model of seismic trace, which according to Usman (2013), states that the seismic trace is the convolution of the reflectivity with a seismic wavelet generated by a source function with addition of noise component. The inversion problem is the opposite process and according Tarantola (2005), consists of using the actual result of some measurements to infer the values of the parameters that characterize a medium, which in case of seismic inversion are elastic parameters of rocks, such as, velocities, density, impedance and porosity.

One of the most useful physical properties in reservoir characterization is acoustic impedance, which is defined by the product between the P-wave velocity and the density of rocks. The acoustic impedance is related to the lithology type, the rock compaction and the existence of fluids in the rock. The inversion process for the acoustic impedance is performed using post-stack data, where initially a log calculated by multiplying density and sonic log is generated. Nevertheless, in the absence of well data, it is possible to generate a pseudo-log by combining the Dix equation to convert the RMS velocity to interval velocity and Gardner's equation to calculate the density.

There are two different approaches to seismic inversion: deterministic and stochastic. According to Francis (2005) deterministic inversion is based on the minimization of an error term between the forward convolution of the reflectivity from an estimated impedance profile and the seismic input data. In each iteration the model is perturbed until a difference close to zero is obtained. There are different methods used to perform the deterministic inversion of acoustic impedance in post-stack data, for example, the classical recursive or band limited, sparse-spike and model-based.

According Russell and Hampson (1991), model-based inversion starts with an initial model, which is adjusted until the synthetic seismic section best fits the acquired seismic data and therefore the error, given by the difference between the synthetic section and the seismic data, is minimized. According to Simm and Bacon (2014) the starting model could be an interpolation of well data (probably with a low-

pass filter applied), a general trend model based on geological model knowledge or the seismic stacking velocity cube. In this inversion the inverted models are a smooth representation of the properties of the subsurface, that compared with the real subsurface properties have less spatial variability (Russell and Hampson, 1991). The advantage of deterministic approaches is the short computation time.

For the stochastic inversion there are two different approaches: The Bayesian algorithms (e.g. Buland and Omre 2003; Buland and El Ouair 2006; Grana and Della Rossa 2010) and the geostatistical inversion algorithms (e.g. Mallick 1995; Mallick 1999; Boschetti, Dentith, and List 1996; Amilcar Soares, Diet, and Guerreiro 2007). Both are optimization processes to solve the inverse problem of the petrophysical parameters, knowing the seismic data. According to Azevedo (2012), the stochastic inversion generates equiprobable outputs of petrophysical properties, such as acoustic impedance, with the main objective to quantify the uncertainty of these properties. The initial model of each realization is obtained through stochastic simulation conditioned to well data and models of the spatial distribution. The average of the equiprobable solutions is defined as the expected value of the given variable. In this approach N iterations are performed, until the correlation coefficient reaches the desired value. In summary, this method aims to minimize the differences between the synthetic seismic traces designated by convolution with the wavelet, and the actual seismic. Once the equiprobable results are obtained, they can be statically analyzed to calculate the variance and to estimate uncertainties and probabilities.

One of the methodologies used in stochastic inversion is the trace by trace methodology, which according to Soares et al. (2007), performs a sequential approach in two steps: first, the acoustic impedance values are simulated for one trace based on well data and information about the spatial continuity given by the variograms, therefore for each simulated trace a synthetic seismogram is generated by using the convolutional model of the seismic trace and compared with the real seismic data. The simulated traces that have a better match with the real seismic are retained and another trace is simulated and transformed. The process continues until all the traces of acoustic impedance are simulated as “real” data for the next sequential simulation step.

A new methodology proposed by Soares et al. (2007) is Global Stochastic Inversion, which is based on two key ideas: the use of the sequential direct co-simulation as the method of “transforming” images, in an iterative process and to follow the sequential procedure of a genetic algorithm optimization to converge the transformed images towards an objective function. This methodology follows a different approach compared to the trace by trace methodologies, because several realization of the entire seismic information of acoustic impedance are simulated instead of individual traces, then a synthetic seismic is calculated for all the simulated images of acoustic impedance and compared with the real data; areas of best fit of different images are selected and a new image is built with the merged information, which is going to be co-simulated in the next iteration. This process is iteratively repeated until obtain a minimum to reach an objective function. At the end are generated

images of the merged of best correlation values and the acoustic impedance values associated to them.

The aim of this project is to explore a hybrid approach by coupling the advantage of deterministic inversion, given by a model-based inversion and a stochastic methodology executed following the geostatistical method, represented by the Global Stochastic Inversion. The available data is a 2D seismic section, which was previously processed to be used in this project, the interval velocity section from processing and interpreted seismic horizons.

The wavelet to be used in both approaches of seismic inversion is extracted from the seismic, considering a statistical method and a minimum phase for the wavelet, because the seismic processing was performed in minimum phase. For the deterministic inversion, a P-wave velocity log is generated from an extracted trace of the interval velocity section, therefore a pseudo log for P-wave impedance is calculated, using Gardner's relationship. For the stochastic inversion, in order to have new pseudo-log with more contribution of the seismic, a new pseudo-log is created extracting a trace from the result of the model-based inversion.

This work has as objective to extend the Global Stochastic Inversion for those cases with lack of well data. The idea is to condition the GSI to prior information, such as probability distribution functions of AI from pseudo-wells and low frequency models. Three cases of conditioning to prior information are considered. Case 1, using a soft-model generated for the execution of the model-based inversion. In the simulation stage is considered a direct sequential simulation taking into consideration this soft-model as local trend (simple kriging with local means, where the local means are set by the soft-model). Case 2, conditioning the GSI with local models of parameters, probability distribution functions and local spatial continuity models (variograms).These models are defined in zones according to the geological interpretation, grouping layers with a similar behavior in the properties. The simulations are performed with a direct sequential simulation using local distributions and local models of variograms of AI. In this case the input for the simulation of the first iteration the same initial soft-model used in the model-based inversion. Case 3, conditioning the GSI to the inverted model resulting from the deterministic inversion. The simulations and the co-simulations are performed using a direct sequential simulation with a simple kriging with local means for the first iteration and after the first iteration using a collocated simple co-kriging with local means, where the best section is used as secondary variable and the result obtained in the deterministic approach is used as image of local means. The idea of this case to use the deterministic inversion as input is to refine the result obtained in the model-base inversion

2. OBJECTIVE

Seismic Inversion allows the transformation of seismic data into quantitative properties of rocks, contributing to the description of the quality of a reservoir, which means that this technique now has an important role in the characterization of reservoirs. In early stages of exploration the use of the seismic inversion process could be limited by the lack of available data, motivating the development of new methodologies in the application of this technique.

Acoustic impedance is a defined as the product between the P-wave velocity and the density of rocks and is related to the lithology, rock compaction and existence of fluids in the rock, which makes this property one of the most useful physical properties in reservoir characterization. Independently of the seismic inversion approach to be followed, it is necessary to have a prior geological knowledge, information about the seismic wavelet and well log data. In case of a deterministic approach the well log data is used to generate an initial model to execute the inversion and for the stochastic approach is necessary to perform a spatial analysis of the distribution of the property. It is important to mention that a good initial model for the seismic inversion should not only be an approximation of the property distribution in the area, also should reflect the geology existing in it.

One of the inputs for the inversion is the seismic wavelet, which can be generated using different techniques. In this case a statistical wavelet with a length of 200ms is extracted from the seismic data, taking into consideration that the processing was performed in a minimum phase. It is important to mention that the extraction is performed in the area of interest.

In this study, to perform seismic inversion in total absence of well data is proposed to create pseudo-logs, task that could be a challenge considering the limitations of the data. One of the techniques used is to create pseudo-logs for P-wave velocity and density calculated from velocity data information. In this case, the P-wave pseudo-log is obtained by the extraction of a trace from the interval velocity section, while the density pseudo-log is generated with the P-wave velocity pseudo log using Gardner's equation. Therefore, the acoustic impedance pseudo-log can be calculated by multiplying the P-wave velocity and the density pseudo-logs. This technique is implemented in this project to generate the pseudo-log for acoustic impedance in a deterministic approach.

Stochastic inversion combines information from well data that offers high resolution vertically, but does not provide lateral information, with seismic data that has the opposite characteristic: densely spaced traces with "limited" vertical resolution. Using the technique described before for the generation of pseudo-logs, the vertical resolution is limited; for that reason, in order to increase it, a different methodology is applied, that follows an optimization approach. This could be achieved in different ways, but for this project, once the results of the deterministic approach have been obtained a trace is

extracted and a new pseudo-log for the acoustic impedance is generated, which due to the seismic contribution reflects the vertical changes of the area in a higher scale.

The stochastic inversion proposed in this study is based on geostatistical techniques and therefore it is necessary to perform an exploratory data analysis to characterize the statistical behaviour of the data. A spatial data analysis is also performed, where the variograms are generated and modelled for the well and for the seismic data, describing the vertical and horizontal behaviour in the spatial distribution of the property to be studied, which in this case is the acoustic impedance.

For the objective of this study the stochastic inversion in an under-sampled reservoir, is performed with a Global Stochastic Inversion technique, following three different new approaches:

1) Using as input a soft-model generated for the execution of the deterministic inversion, considering a direct sequential simulation with local mean for the simulation stage. The inputs for the GSI are the pseudo-log of acoustic impedance, the parameters used to model the vertical and horizontal variograms and the soft-model. In this case the local means in the simulation are set by the soft-model.

2) Using a model divided by zones according to the geological interpretation, grouping layers with similar lithological characteristics and performing the simulations with simple kriging with local mean. The inputs of the GSI are a model of zones, the pseudo-log, which should have a division by zones as well, the maximum and minimum values of the property for each zone, the parameter used to model the variogram and a soft-model represented by the initial model of the deterministic inversion. In this case the local means are set by the local distributions of the property in each zone.

3) Using as input the output from the deterministic inversion. The inputs of the GSI are the pseudo-log of acoustic impedance, the parameters used to model de vertical and horizontal variograms and output of the deterministic inversion, which represents the soft-model. The simulations and the co-simulations are performed using a direct sequential simulation with a simple kriging with local means for the first iteration and after the first iteration using a collocated co-kriging with local means, where the best section is used as secondary variable and the result obtained in the deterministic approach is used as image of local means. The idea of this case to use the deterministic inversion as input to refine the result obtained in the model from the deterministic approach.

It is important to mention that the results allow an assessment of the uncertainty, which is important because it gives an idea of the confidence in the estimated values. The assessment of the uncertainty represents an advantage of the stochastic methodologies against the deterministic.

The main advantage of the GSI is that it does not need log data in the area to be inverted; it is possible to use logs from other places with a similar geology. The final results of this project show another important advantage of the GSI regarding the quality of seismic data, which is that in zones where the quality of the seismic data is doubtful the variability of final acoustic impedances images is high, which means that these are poorly matched at the end of the inversion process, by not forcing

the inversion to reproduce the seismic in the area and therefore not reproducing the noise in the final result. These reasons make the GSI a technique suitable to be applied in under-sampled reservoirs, where the quantity of data is limited and by being in early exploration stages the quality of the seismic data could be poor.

2. THEORETICAL FRAMEWORK

3.1 Seismic reflection methods

The reflection of a wavelet occurs when the medium does not absorb it, producing the return or rebound of the energy. The reflection is produced as a consequence of the acoustic impedance contrast between two media (Figure 1), which is given by the product between the compressional-wave velocity and the bulk density.

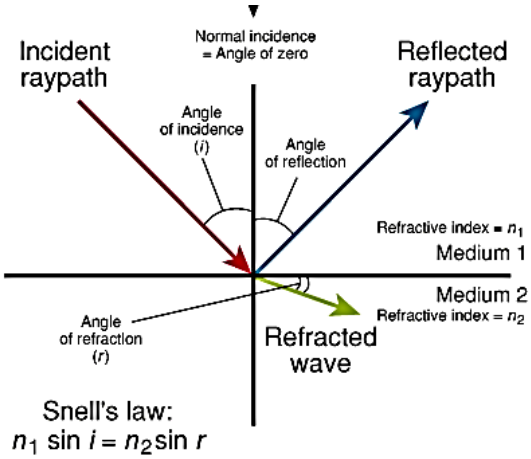

Figure 1. Diagram of reflection and refraction.
(Source: http://www.glossary.oilfield.slb.com/en/Terms/r/reflection.aspx)

The seismic reflection method is a geophysical method which records at the surface the acoustic waves that were reflected from different interfaces (reflectors), where there are significant changes of the material density or in the wave propagation velocity. As a result is obtained a seismic section which, after adequate processing, generates an approximation of the subsurface structure. This method is widely used in hydrocarbon exploration and production because it has a great power of resolution and penetration. In seismic data acquisition the technique consists of generating seismic waves by using sources of energy such as explosives and Vibroseis, and to measure with recording equipment the travel time of the waves from the generation until its reception at sensors (geophones and hydrophones) placed on the surface or underwater. Therefore, with the travel times and knowing the velocities of propagation it is possible to do a reconstruction of the trajectories of seismic waves. The travel time depends on factors such as the physical properties of the rocks, the structural geology of the area and the fluid content.

There are different applications of seismic reflection acquisition depending on the maturity of the exploration in a certain area, from purely exploration to field production monitoring:

- **2D seismic acquisition**. In 2D seismic acquisition, seismic reflection profiles are acquired, the source that generates the seismic waves and the receivers responsible for recording are localized in the same line. In a 2D survey, the seismic lines are acquired individually with regular or irregular gaps between the adjacent lines, usually with numerous lines acquired in the dip direction, perpendicular to the main geological trends, which could be prospective zones, and fewer lines in the strike direction to the geological structures to make possible the seismic interpretation and structural mapping of the area.
- **3D seismic acquisition**. In this approach is performed a simultaneous acquisition of spatially very dense 2D seismic lines, which make it possible to obtain a volume of tridimensional data (e.g. data spaced by 12.5mx25m).
- **4D seismic acquisition**. In this case a 3D seismic acquisition is performed at different periods of time (a baseline at T0 and another 3D after x years of field production, T1), the aim is to carry out monitoring of a reservoir and to study the evolution of the fluid movements and pressure changes over time using the properties and seismic attributes.

3.2 Seismic reflection coefficient

The reflection coefficient describes the amplitude of the reflected wave in relation with the amplitude of the incident wave.

3.2.1 Reflection coefficient in a normal incident case.

In a normal incidence case, the reflection coefficient of a P-wave is:

$$Ro = \frac{I_2 - I_1}{I_2 + I_1} = \frac{\rho_2 V_2 - \rho_1 V_1}{\rho_2 V_2 + \rho_1 V_1} \quad (1)$$

Where,

R is the reflection coefficient

I_1 and I_2 are the acoustic impedance of medium 1 and medium 2

ρ_1 and ρ_2 are the density of medium 1 and medium 2

V_1 and V_2 are the velocity of medium 1 and medium 2

The reflection coefficient has values between -1 and 1. A negative value indicates a phase change of 180º in the reflected wave.

3.2.2 Zoeppritz equations

For non-normal incidence, the reflection coefficient is calculated with the Zoeppritz equations, which according to Aki and Richards (1980), these equations describe the partitioning of energy among

reflections and transmissions of compressional and shear waves at an interface at an interface, which is consider to be plane and uniform.

3.2.3 Approximations of the Zoeppritz equations.

The Zoeppritz equations are complicated and difficult to manipulate, for this reason generally they are applied in a simplified form. One of these forms is the Aki & Richards approximation, published in 1980. This approximation is based in the following assumptions:

- The percentage changes in elastic properties are small.
- The reflection coefficient for the normal incidence case is small.

Mathematically, the approximation is given by the following expression:

$$R(\theta) = \frac{1}{2}\left(1 - \frac{4\beta^2}{\alpha^2}\sin^2\theta\right)\frac{\Delta\rho}{\rho} + \frac{1}{2cos^2\theta}\frac{\Delta\alpha}{\alpha} - 4\frac{\beta^2}{\alpha^2}sin^2\theta\frac{\Delta\beta}{\beta} \quad (2)$$

In 1985 Shuey modified the Aki & Richards equation, rearranging algebraically the terms according to their angle-range contribution to the reflection coefficient. According to Chopra (2014) the first term is related with the contribution of the normal incidence reflection coefficient, the second term is given by the difference in Poisson's ratio, and has influence in middle angles of incidence, between 15 and 30 degrees, and the third term is significant only if the variations in velocity are large. Shuey's approximation is given by:

$$R(\theta) = Ro + Gsin^2\theta + F\ (tan^2\theta - sin^2\theta) \quad (3)$$

Where Ro is the reflection coefficient for P-wave at normal incidence and θ is the angle of incidence. Parameters G and F are calculated from:

$$G = \frac{1}{2}\frac{\Delta Vp}{Vp} - 2\frac{Vs^2}{Vp^2}\left(\frac{\Delta\rho}{\rho} + 2\frac{\Delta Vs}{Vs}\right) \quad (4)$$

$$F = \frac{1}{2}\frac{\Delta Vp}{Vp} \quad (5)$$

Where:

Vp and ΔVp are the average and the difference of P-wave velocity between two mediums

Vs and ΔVs are the average and the difference of S-wave velocity between two mediums

ρ and $\Delta\rho$ are the average and difference of density between two mediums

In equation 3, Ro represents the AVO intercept attribute, controlled by the contrast in acoustic impedance and related with near-offsets and G is the AVO gradient attribute. By assuming that the angle of incidence is less than 30º, *F* tends to zero and equation 3 is simplified to:

$$R(\theta) = Ro + Gsin^2\theta \tag{6}$$

3.3 Gardner's equation

Gardner's equation states a relationship between bulk density (ρ) and P-wave velocity (Vp). It is described by:

$$\rho = \alpha Vp^{\beta} \tag{7}$$

Where α and β, are empirical derived constants and depend on the geology and can be calculated using well log information, but in the absence of well information can default Gardner's constants may be used. Constant β is equal to 0.25 and α has different values depending on the units of Vp (the density is always expressed is g/cc). If Vp is in m/s, α has a value of 0.31 and in case of Vp is in ft/s, α is equal to 0.23.

Boore (2007) describes this relation as "*an approximate average of the relations for a number of sedimentary rock types, weighted toward shales".* The relationship, for Vp in ft/s is shown graphically in Figure 2 (dashed line).

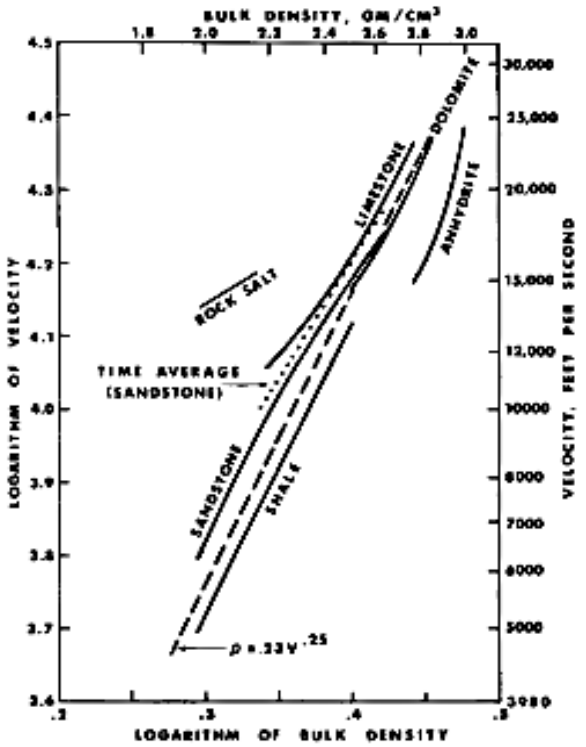

Figure 2. Velocity-density relationship in rocks of different lithology (Source: Gardner et. al.1974)

Substituting the Gardner's constants and multiplying both sites of the equation by the interval velocity will give the acoustic impedance:

$$I = 0.31Vp^{1.25} \quad (8)$$

3.4 Wavelet extraction methods

The wavelet is defined as a "one-dimensional pulse, usually the basic response from a single reflection coefficient reflector. Its key attributes are its amplitude, frequency and phase". The wavelet is originated by a source (e.g. dynamite and Vibroseis), in a specific time and at longer travel times has less high frequency relative to low frequencies. Wavelet energy decays with time as more partitioning takes place at interfaces (Oilfield Glossary).

The wavelet extraction is a complex methodology and is an important step in the inversion process. Although numerous wavelet extraction methods have been devised, the following general statements can be made:

The wavelet extraction problem consists of two parts:

1) Determine the amplitude spectrum
2) Determine the phase spectrum

Of these two, determining the phase spectrum is by far the more difficult and presents a major source of error in inversion.

The wavelet extraction methods can be divided into three major categories:

a) **Purely deterministic:** This means measuring the source wavelet using nearby surface receivers.

b) **Purely statistical:** This means determining the wavelet from the seismic data alone. Purely statistical methods use the autocorrelation of the seismic traces over a small window to estimate the amplitude of the wavelet. These procedures tend to have difficulty determining the phase spectrum reliably. According to the STRATA user's guide (1999) the steps following during the statistical wavelet extraction for each trace in an analysis window are:

1. Extract the analysis window
2. Taper the start and end of the window with a taper length equal to the lesser of: 10 samples, ¼ of the window.
3. Calculate the autocorrelation of the data window.
4. Calculation of the amplitude spectrum of the autocorrelation and take the square root of it, which approximates the amplitude spectrum of the wavelet.
5. Add the desired phase.

6. Calculate the inverse Fast Fourier Transform to produce the wavelet.

Finally the wavelets calculated from the traces in the analysis window are summed.

c) **Use a well log:** This means using well-log information in addition to the seismic data. In theory, this could provide exact phase information at the well location. The problem is that this method depends critically on a good tie between the log and the seismic. In particular, the depth-to-time conversion, which converts the depth sampled log to two-way travel-time, can cause misties that could degrade the result.

Wavelets are not constant from trace to trace and as function of travel-time. In theory, the idea is to extract a wavelet varying in space and time, but in practice a single average wavelet is extracted and used for the impedance inversion.

3.5 Convolutional model of the seismic trace

The convolutional model of the seismic trace is defined by the following relation:

$$x(t) = w(t) * r(t) + n(t) \quad (9)$$

Where $x(t)$ is the seismic trace, which is equal to the convolution of a band limited wavelet $w(t)$ with the reflectivity series $r(t)$ and the addition of random noise n that could be in the recorded seismic. According to Yilmaz (1987) this model assumes:

- The Earth is made up of horizontal layers of constant velocity.
- The source produces a compressional plane wave, which meets the layers boundaries at normal incidence.
- The source waveform is stationary, this means that does not have loss of amplitude by spreading or absorption.
- The wavelet generated by the source is known.

3.6 Geostatistics

Geostatistics is a technique that provides a formal basis to perform the description, simulation and estimation of the spatial and temporal distribution of a natural phenomenon. In Geophysics this technique could be applied to characterize physical properties of rocks, for example elastic parameters, properties of a reservoir, such as lithology and porosity. This technique is important in the construction of earth models and was initially developed by Matheron in the sixties and applied to the mining industry and adopted by the petroleum industry in the eighties following the pioneering work of Andre G. Journel. The goals of the geostatistical methods are the estimation of the most probable value and the estimation of the uncertainty of the predicted values. Some of the concepts applied in Geostatistics and used in this work are described on the following sub-sections.

3.6.1 Random variable.

A variable whose values are generated according to some probabilistic mechanisms. This variable takes a range of possible values according to a Probabilistic Distribution Function or PDF. A random variable could be continuous or discrete; in the first case the variable has continuous range of possible values and in the second case the values are limited or finite. A set of correlated random variables forms a random function.

3.6.2 Mean and Variance.

According to Soares (2000) given a random variable, the mean is weighted average of possible values that the random variable can take. The mean is given by:

$$m(x_i) = E\{z(x_i)\} = \int_{-\infty}^{\infty} z \, dF_{xi}(z) \tag{10}$$

Where x_i is the spatial localization of a value, $z(x_i)$ is a realization of the random variable Z, $E\{z(x_i)\}$ denotes the expected values and $F_{xi}(z)$ represents probabilistic distribution function of the random variable.

Assuming stationarity in the mean value, which means that for all the random variables is the value is the same independent of the localization, the mean can be calculated as an arithmetic mean of the realizations of the random variables:

$$m = \frac{1}{N}\sum_{\alpha=1}^{N} Z(x_\alpha) \tag{11}$$

The spread of the values around the mean is measures by the variance, which mathematically is expressed with the following equation:

$$\sigma^2 = E[(z - m(x_i)^2] = \int_{-\infty}^{\infty}(z - m(x_i)^2 dF_{xi}(z) \tag{12}$$

3.6.3 Variogram and Covariance

The variogram and the covariance are measures of the correlation between two random variables. Assuming that the correlation is only dependent upon the spatial distance between the variables and it is independent of the localization of the variables (stationarity hypothesis):

$$C(Z(x_1), (Z(x_2)) = C\left(Z(x_i), (Z(x_i + h))\right) = C(h) \tag{13}$$

$$\gamma(Z(x_1), (Z(x_2)) = \gamma\left(Z(x_i), (Z(x_i + h))\right) = \gamma(h) \tag{14}$$

Where $C(h)$ represents the covariance and $\gamma(h)$ is the variogram, which makes possible the description of quantitative variation in the space of a regionalized variables. The variogram function is defined by:

$$\gamma(h) = \frac{1}{2N(h)} \sum_{\alpha=1}^{N(h)} [Z(X_\alpha) - Z(X_\alpha + h)]^2 \quad (15)$$

And the not centered covariance is expressed by:

$$C(h) = \frac{1}{N(h)} \sum_{\alpha=1}^{N(h)} [Z(X_\alpha)\, Z(X_\alpha + h)]^2 \quad (16)$$

The relationship between the variogram and the covariance is:

$$\gamma(h)) = C(0) - C(h) \quad (17)$$

Figure 3 represents the relationship between the variogram and the covariance, where it is possible to observe that the variogram increases with distance, because it is a measure of the dissimilarity between data values as a function of the distance. On other hand the covariance tends to decrease with the distance, being a measure of the similarity between the values. The variogram has a correlation range, beyond this range the data values are uncorrelated and the variogram reaches a plateau level which is called the sill; if the property has high spatial continuity the range will be high as well and reach the sill slowly. The sill is related with the variability of the data.

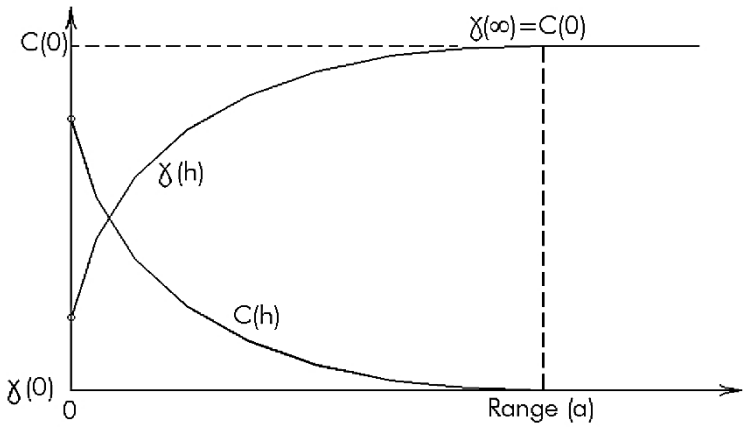

Figure 3. Relationship between the Covariance and the Variogram (Source: http://www.minetechint.com/papers/droy-thesis/)

3.6.4 Theoretical models of variograms

The experimental variogram can be adjusted to positive functions, for example spherical models, exponential and Gaussian.

Spherical model. According to Soares (2000), this model is the most widely used model in geostatistics and it is function of two parameters: the sill, which represents the maximum value of the variogram and the amplitude a, which is the distance at which the values of $\gamma\ (h)$ stop to increase and are equal to the sill, which is normally coincident with the variance of the random variable. Mathematically is expressed by:

$$\gamma\ (h) = \begin{cases} C\left[1.5\ \frac{h}{a} - 0.5\left(\frac{h}{a}\right)^3\right] & para\ h \leq a \\ C & para\ h > a \end{cases} \quad (18)$$

Exponential model. This model initially growths faster than the spherical, but has highest correlations with big distances *h*, therefore the structures have more spatial continuity. This model is defined by:

$$\gamma(h) = \ C\left[1 - e^{\frac{-3h}{a}}\right] \quad (19)$$

It is important to mention that both functions, shown before, spherical and exponential are used to model irregular phenomena.

Gaussian model. This function is used for regular phenomena that has a slow growth of $\gamma\ (h)$ with a parabolic behavior in the origin. This case is used to model variables with more spatial continuity compared to the models shown before. This model is given by:

$$\gamma(h) = \ C\left(1 - exp^{\left(\frac{-3h^2}{a^2}\right)}\right) \quad (20)$$

3.7 Linear estimation: Kriging

According to Doyen (2007), Kriging is an interpolation technique developed by George Matheron in 1965 in recognition of the work performed by Daniel Krige in the mining industry. Kriging is used to estimate the values of a property at one unmeasured location through the linear combination of observed values of the property at surrounding locations. The estimated value is a weighted sum of the known values and the weights depend on the separation distance between them. The ordinary kriging estimator is defined by:

$$Z\lceil(x_o)\rceil^* = \sum_{\alpha=1}^{N} \lambda_\alpha Z(x_\alpha) \quad (21)$$

Where $Z\lceil(x_o)\rceil^*$ represents the estimates at the unsampled or unmeasured location x_o, λ_α=1… N are the weights of the values of the property $Z(x_\alpha)$ at the surrounding locations x_α. This estimator is not unbiased, in other words the $E\{\varepsilon(x_O)\} = Z\lceil(x_o)\rceil^* - Z(x_o) = 0$. The estimator also has a minimum error variance, $\min\{var(\varepsilon(xo))\}$. It is important to mention that in the case of ordinary kriging the

mean values of the random variables are known and spatially constant, being the stationary case of kriging.

3.7.1 Simple Kriging

According to Soares (2006), simple kriging is the most general version of non-stationary kriging, in which the knowledge of the mean values of the set of random variables relative to the unsampled points are assumed. The non-stationary means that for this estimator the mean value is not constant. Equation 22 shows the estimator for the simple kriging with locally variable mean:

$$Z\lceil(x_o)\rceil^* - m(x_o) = \sum_{\alpha=1}^{N} \lambda_\alpha [Z(x_\alpha) - m(x_\alpha)] \quad (22)$$

The mean in each location is estimated prior to kriging and is used as secondary information. Assuming the stationarity of the mean, equation 21 can be expressed as:

$$Z\lceil(x_o)\rceil^* = m + \sum_{\alpha=1}^{N} \lambda_\alpha [Z(x_\alpha) - m] = \sum_{\alpha} \lambda_\alpha Z_\alpha + \ [1 - \sum_{\alpha=1}^{N} \lambda_\alpha] m \quad (23)$$

In this case the mean does not depend on the location and represents global information for all the unsampled locations.

3.7.2 Co-kriging

This technique incorporates in the estimation the use of one or more secondary variables, which must be correlated with the primary variable. The secondary variable has a higher sampling density than the primary variable. In this case the estimator in a specific location x_o is given by:

$$Z_1\lceil(x_o)\rceil^*_{CK} = \ \sum_{i=1}^{N1} \alpha_i Z_1(x_i) + \sum_{j=1}^{N2} \beta_j Z_2(x_j) \quad (24)$$

Equation 24 represents the linear combination of the neighboring values of both variables, the primary Z_1 and the secondary variableZ_2.

3.7.2 Collocated co-kriging

According to Soares (2006), collocated co-kriging is a technique used when the density of the secondary variable is overabundant relative to the primary variable, which is solved using only the value of the secondary variable in the point to be estimated. In these cases the co-kriging is unstable and the correlation between two neighboring values to the variable could be much higher than the correlation between two values that are next to the principal variable. The collocated co-kriging estimator is defined by:

$$Z_1\lceil(x_o)\rceil^*_{CK} = \ \sum_{i=1}^{N1} \alpha_i Z_1(x_i) + \beta_o Z_2(x_o) \quad (25)$$

Where Z_1 is the primary variable, $Z_1(x_0)$ is the estimated value of the primary variable at a given position x_0, primary variable and $Z_2(x_0)$ is the value of the secondary variable at a given position x_0.

3.8 Geostatistical simulation

The principal objective of geostatistical simulation models is to generate equiprobable images of the reality and to integrate the concept of uncertainty in stochastic models of high resolution. Simulation models respect the spatial variability, represented by the variogram, the global probability distribution function or histogram and the experimental data, which means that the data should pass through the experimental points.

3.9 Seismic inversion

According to Tarantola (1987) the forward problem is defined as the prediction of the result of measurements, giving a complete description of a physical system, this is used to generate synthetic data. The inversion process is defined as the reconstruction of a model of parameters or properties of the medium involved from a set of measurements or observed data, which represents the response to a stimulus or perturbation induced in it (Figure 4). In the case of seismic inversion the model of parameters is formed by elastic parameters of rocks, such as, velocities, density, impedance or porosity and the perturbation is caused by a seismic wave. Is important to mention that the seismic inversion methods are based on the convolutional model of the seismic trace described before.

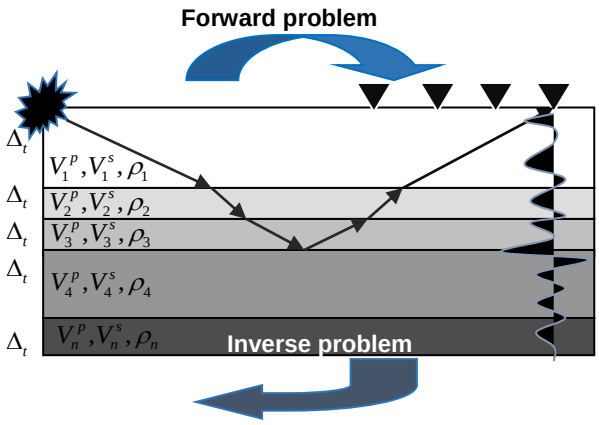

Figure 4. Forward and **Inverse problem.**

Seismic inversion methods have different approaches, deterministic and stochastic. According to Francis (2005), the deterministic approach is based on the minimization of an error term between the forward convolution of the reflectivity from an estimated impedance profile and the seismic amplitudes at each trace location. The stochastic approach is based on the generation of equiprobable solutions and the average of all solutions is defined as the expected value.

3.9.1 Deterministic Inversion

Deterministic inversion is an optimization technique, which aims to improve, iteratively a particular model, looking forward to maximize the probability density function and therefore minimize the difference of the model with the real model. In each iteration the model is perturbed until a difference

close to zero is obtained. According to Hampson and Russell (1991) for post-stack data the deterministic inversion could be grouped in three categories: classical recursive or band-limited, sparse-spike and model-based.

3.9.1.1 Band-limited inversion

Band-limited inversion or recursive inversion was developed in 1979 by Lindseth and is the first type of post-stack inversion developed. In this inversion the result has the same frequency band as the seismic data, losing the low and high frequency detail provided by the logs. The technique is based on the assumption that the seismic trace represents an approximation to the reflectivity of the Earth and therefore this can be inverted to obtain the acoustic impedance. The reflectivity trace is calculated by the deconvolution of the seismic trace with the inverse wavelet and after this the conversion of the reflectivity trace to an impedance trace is performed. The disadvantage of this methodology is that the seismic trace has a band-limited nature, with frequencies that go typically from 10 to 60 Hz, with missing or poorly determined values in the low frequency band and in the high frequency band.

3.9.1.2 Sparse-spike inversion

According to Gavotti (2014) sparse-spike inversion estimates a set of sparse reflection coefficients from the seismic data and constrains them with the model to produce the impedance from inverting these coefficients. This method is broad-band and generates a model with high frequency. The disadvantage is that the events should match with the seismic trace and therefore the results could simplify the geology, having less events. There are generally two algorithms used to perform this inversion, linear programing and maximum likelihood. This type of inversion is not model dependent, being suitable for zones with poor knowledge of the geology and is the best method to use in areas with fewer reflectors.

3.9.1.2 Model-based inversion

Model-based inversion starts with a subsurface model, which is perturbed to minimize the error between the synthetic derived from this model and the original seismic data. According to Simm and Bacon (2014) the starting model could be an interpolation of well data (probably with a low-pass filter applied), a general trend model based on geological model knowledge or the seismic stacking velocity cube. In this inversion the inverted models are a smooth representation of the properties of the subsurface, that compared with the real subsurface properties have less spatial variability (Russell and Hampson, 1991).

According to Gavotti (2014), this type of inversion uses a generalized linear inversion algorithm (GLI), which assumes that the seismic trace (T) and the wavelet (W) are known and the noise is random and uncorrelated with the signal. The initial model is iteratively modified, until match is obtained between the synthetic derived from the model and the real seismic data. The approach of the model is to minimize the function:

$$J = weight_1 x(T - W * r) + weight_2 x(M - H * r) \quad (26)$$

Where, T is the seismic trace, W is the wavelet , r is the final reflectivity, M the initial guess model impedance and H is the integration operator which convolves the final reflectivity to produce the final impedance. By the minimization of the first part of the equation the solution that models the seismic trace and minimizing the second part forces a solution that models the initial guess impedance. The weights are going to determine the balance between the contribution to the final result of the seismic data and the initial model.

Figure 5 shows the flowchart of the model-based inversion, assuming that the input data is post-stack and the property being inverted is the acoustic impedance. The model trace is simulated calculating a synthetic seismic trace, using the initial impedance low frequency model and the extracted seismic wavelet. The synthetic trace is compared with the input seismic trace. If the error is small enough, the solution is the estimated model trace and the algorithm finishes the iterative process with that trace and continues with the next trace, otherwise an update is calculated in the impedance model and all the process is repeated.

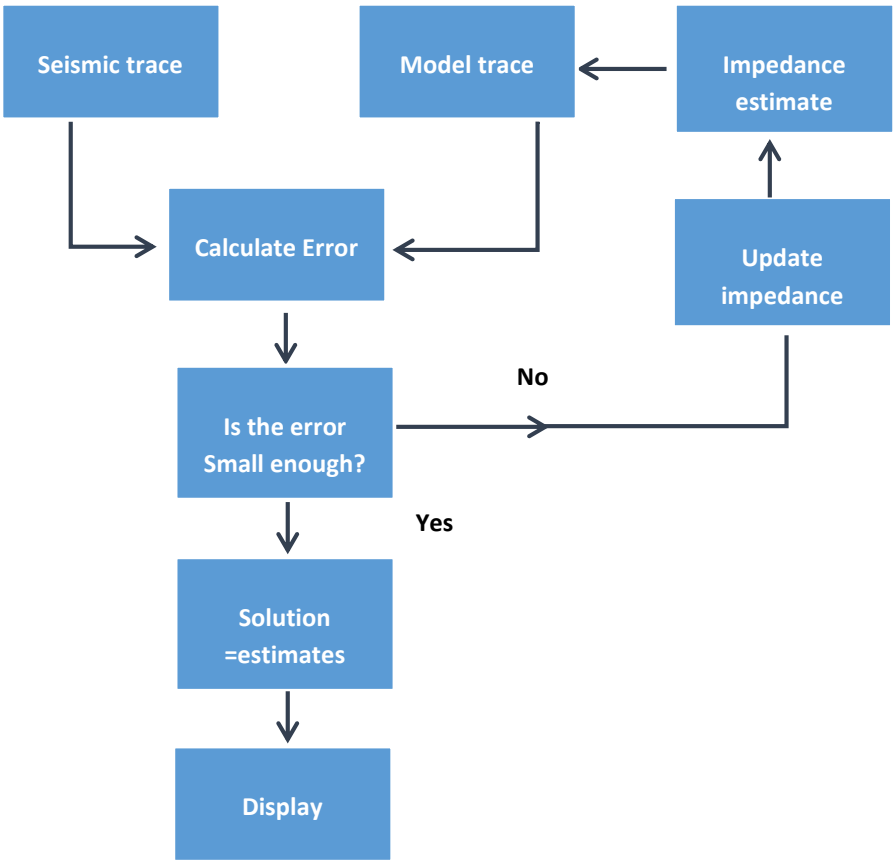

Figure 5. Model-based Inversion (Modified from: Russell, B. 1988).

3.9.2 Stochastic inversion

Seismic stochastic inversion generates equiprobable outputs of petrophysical properties, such as the acoustic impedance, with the main objective to quantify the uncertainty of these properties (Azevedo et al, 2012). The initial model of each realization is obtained through stochastic simulation conditioned to well data and models of the spatial distribution.

The fact that there are equiprobable outputs implies that different realizations give acceptable solutions to the convolution of the reflectivity series with a wavelet compared with the observed seismic. A stochastic methodology demands all possible and acceptable solutions to the acoustic impedance and the average between all solutions is considered as the expected value of a given variable.

In this approach are performed N iterations, until the correlation coefficient reaches the desired value. In summary, this method aims to minimize the differences between the synthetic seismic traces designated by convolution with the wavelet, and the actual seismic. Once the equiprobable results are obtained, they can be statically analyzed to calculate the variance and to estimate uncertainties and probabilities.

3.9.2.1 Trace by trace geostatistical inversion methodologies

In this approach, each trace of the seismic information is visited individually following a random path previously defined. In each point of the random path N realizations of the acoustic impedance are performed, taking into consideration the well log data and the previously simulated traces. By the calculation of the reflection coefficients for one trace and convolving these with an input wavelet is simulated a synthetic seismic trace in each location, which is compared to the real seismic to obtain the correlation coefficient; this is performed for each realization. The realization of acoustic impedance with the highest correlation coefficient is used as conditioning data in the simulation of a next acoustic impedance trace in the random path.

One of the limitations of this method is that in zones with a low signal-to-noise ratio the trace is forced to fit to the seismic data, which is going to be used to condition the next simulation at a new location and therefore noisy values are propagated. To overcome this limitation in more recent versions of this technique, is omited the location where the correlation is between the synthetic trace and the real seismic trace is low and re-visited in late stages of the inversion procedure.

3.9.2.2 Global Stochastic Inversion (GSI)

Global stochastic inversion follows a different approach; in this methodology several realizations of the entire seismic information of acoustic impedance are simulated instead of individual traces, then synthetic seismic is calculated for all the simulated images of acoustic impedance and compared with the real data; areas of best fit of different images are selected and a new image is built with the merged information, which is going to be co-simulated in the next iteration. This process is iteratively

repeated until obtain a minimum to reach an objective function. At the end are generated images of the merged of best correlation values and the acoustic impedance values associated with them. Figure 6 represents a schema of the GSI process:

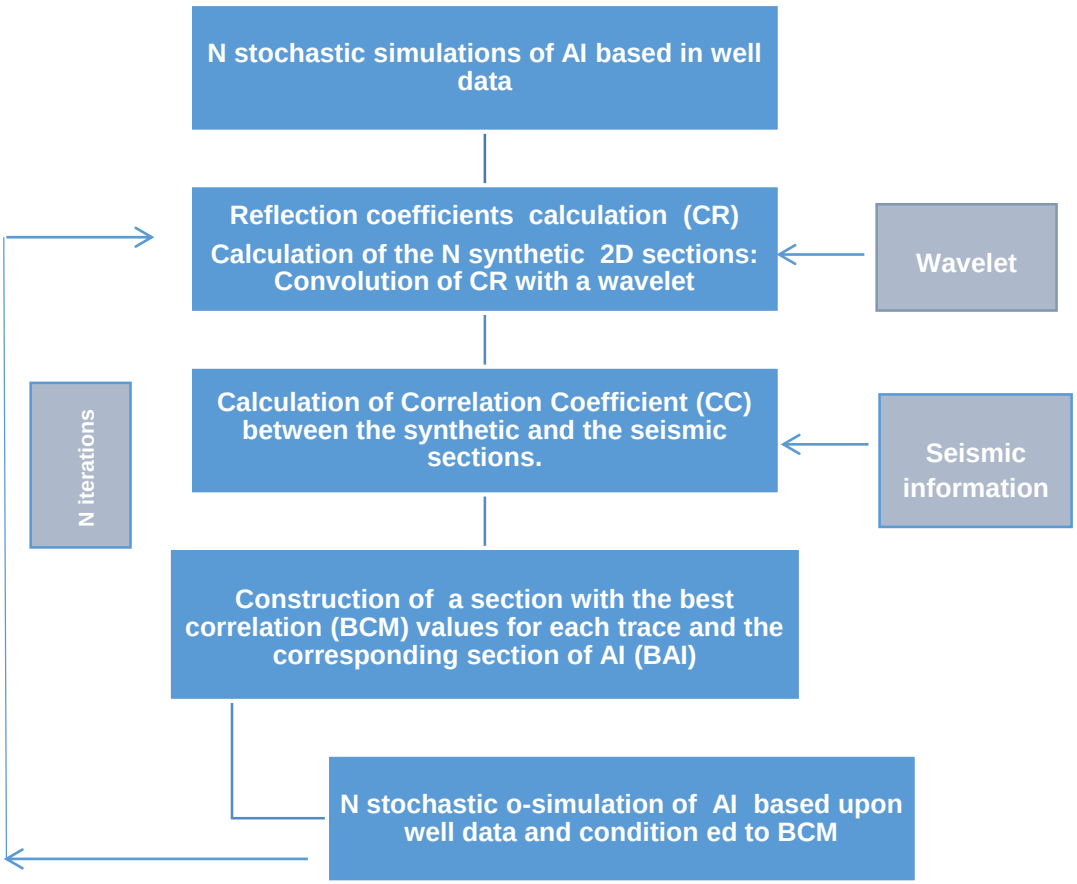

Figure 6. Stochastic Inversion

The advantage of this technique compared with techniques of trace by trace inversion is that in zones when the signal-to-noise ratio is low the final inversion results remain poorly matched and do not force the inversion to reproduce the seismic data. At the end of the inversion process these areas are going to have a high variability or uncertainty.

4. METHODOLOGY

In this section are described the methodologies used for both approaches of seismic inversion considered in this project, a deterministic approach performed with a Model-based inversion and a stochastic approach based on a Global Stochastic Inversion. The available data are in figures 7 and 8, where it is possible to observe the final stack of a 2D line with the horizons provided by the interpreter and the final interval velocity section from seismic processing. For this project no well information is available.

The outputs in both approaches are going to be sections of acoustic inversion for P-impedance. It is important to mention that the seismic processing from field data to pre-stack time migration, was designed and performed as part of this project and the processing sequence and some results are available in the appendix section. The data consists of a 2D line with 5194 CDP's with a distance of 12.5 meters between each CDP and the sampling rate is 4 ms. The record length is 8192 ms, but for practical reasons the inversions were performed in a window between 1000 ms and 4300 ms, which is the target zone.

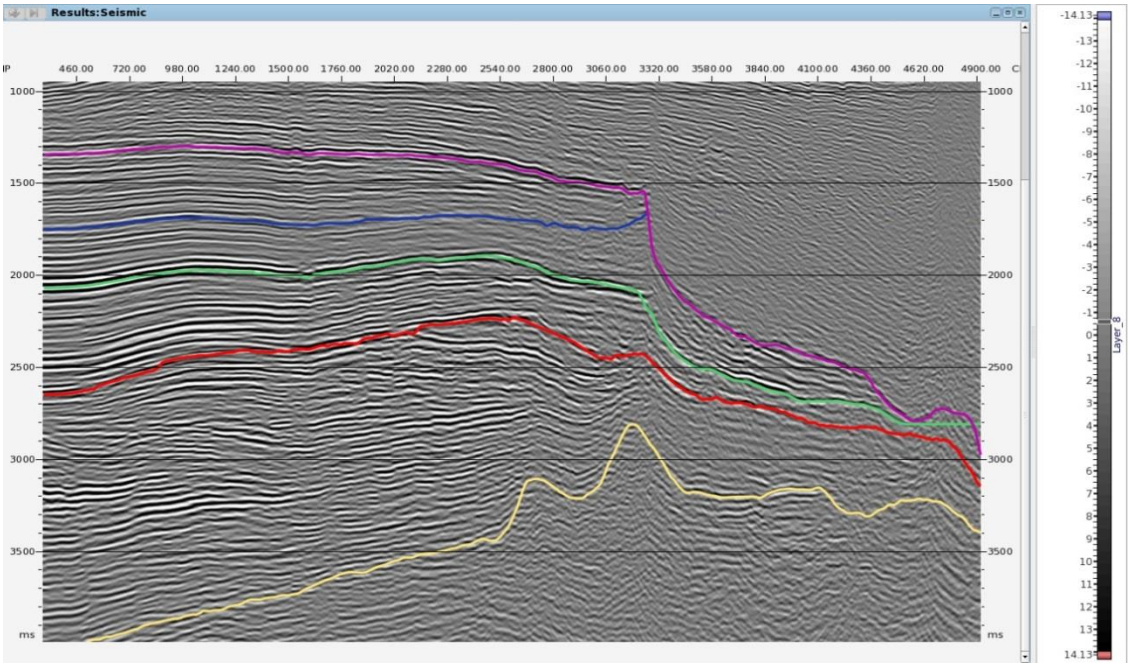

Figure 7. Final PSTM from processing - interpreted.

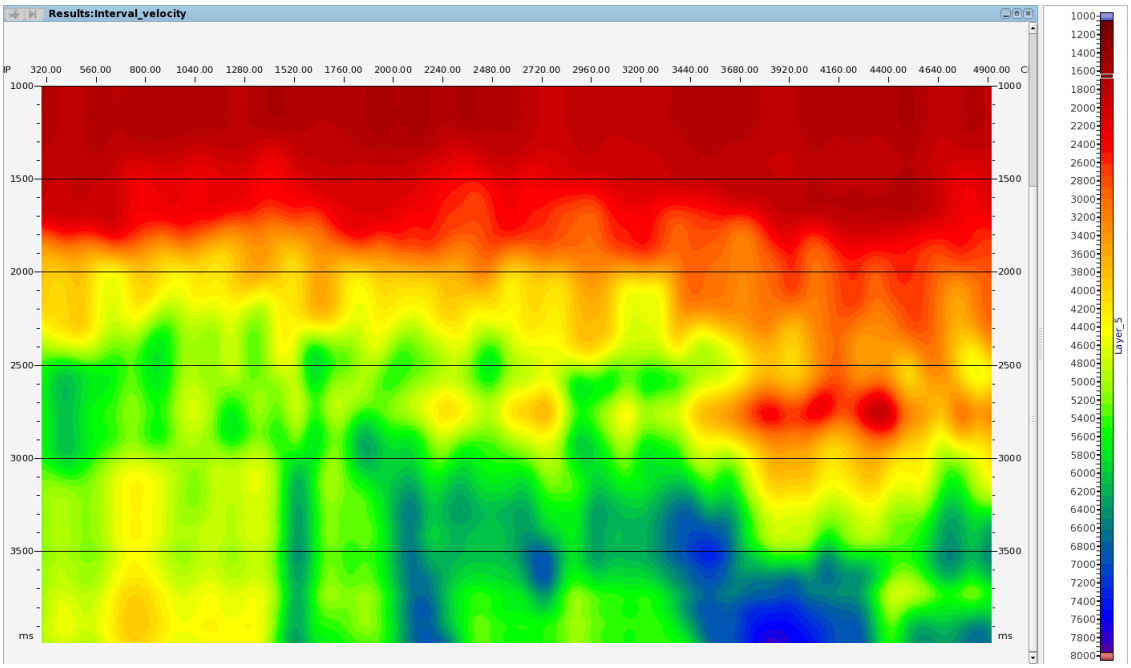

Figure 8. Final interval velocity section.

4.1 Model-based Inversion

The Model-based Inversion was performed using Strata from CGG Hampson-Russell, which is a software widely used in the industry implemented to perform seismic reservoir characterization. This type of inversion needs as input the seismic data, a wavelet, interpreted horizons and well logs. The software has the option to extract a statistical wavelet from the seismic, in this case a wavelet with a length of 200ms and minimum phase was extracted, because the seismic processing was performed in minimum phase. In figure 9 is the extracted wavelet:

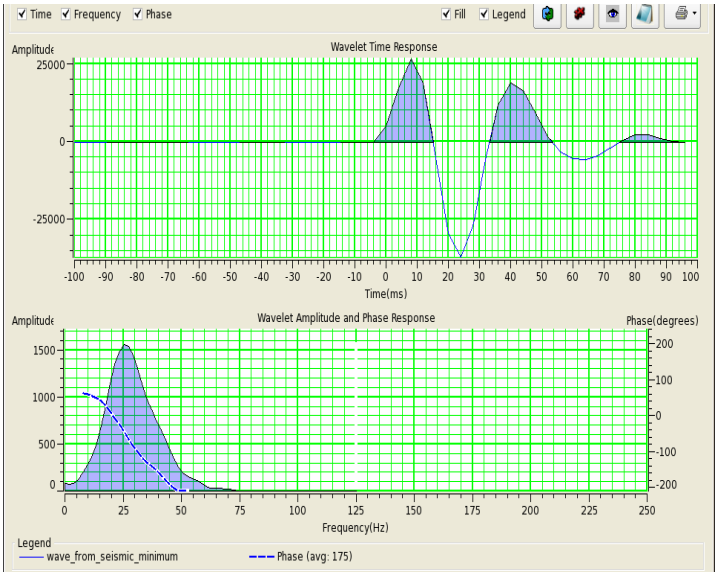

Figure 9. Extracted wavelet

It is important to point out that as the wavelet can change from trace to trace and as function of travel time, it was necessary to perform the statistical extraction in the target zone; this could help to have a better estimation of the synthetic and therefore to have a more reliable result.

As was mentioned before in this case well data was not available, for that reason it was necessary to create pseudo logs of P-wave velocity and density, which are a requirement of the software. The P-wave velocity log was obtained by the extraction of a trace from the section of interval velocity and the density log was calculated using the Gardner relationship (eq. 8). After calculating the pseudo logs for P-wave velocity and density, it is possible to generate a pseudo log for acoustic impedance, which is going to be used in the inversion process.

Figure 10 shows the pseudo logs for P-wave velocity, density and impedance generated. The pseudo-log for P-wave velocity has values between 3883 m/s and 6277 m/s, the pseudo-log calculated for the density has values between 2.5 g/cc and 2.76 g/cc and pseudo-log derived for P-wave impedance has values between 10547 (m/s)*(g/cc) and 17319 (m/s)*(g/cc).

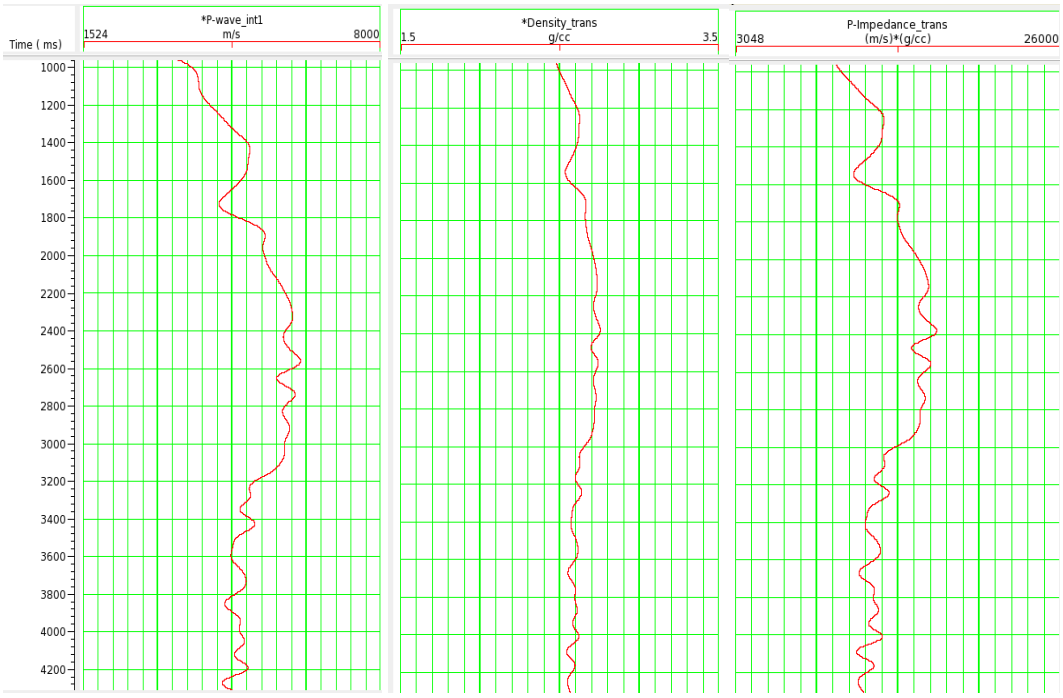

Figure 10. Pseudo-wells of P-wave velocity, density and P-impedance

This inversion has as an input an initial model, which should reflect the geological structure of the area and has an approximation to the real values of the property. Usually this is created by interpolating the values of the well data of the property to invert; this interpolation is guided by the interpreted horizons. The well data has a higher resolution compared with the seismic data and applying a low pass filter, permitting a maximum frequency between 10 and 15 Hz, generating then a low frequency mode. In

this case due the absence of data, the initial model was generated by extrapolating the values of the pseudo-log of acoustic impedance and taking into consideration the horizons previously interpreted; this data is already low frequency and for that reason it was not necessary to apply a high-cut filter in the model. Figure 11 shows the initial model of the inversion.

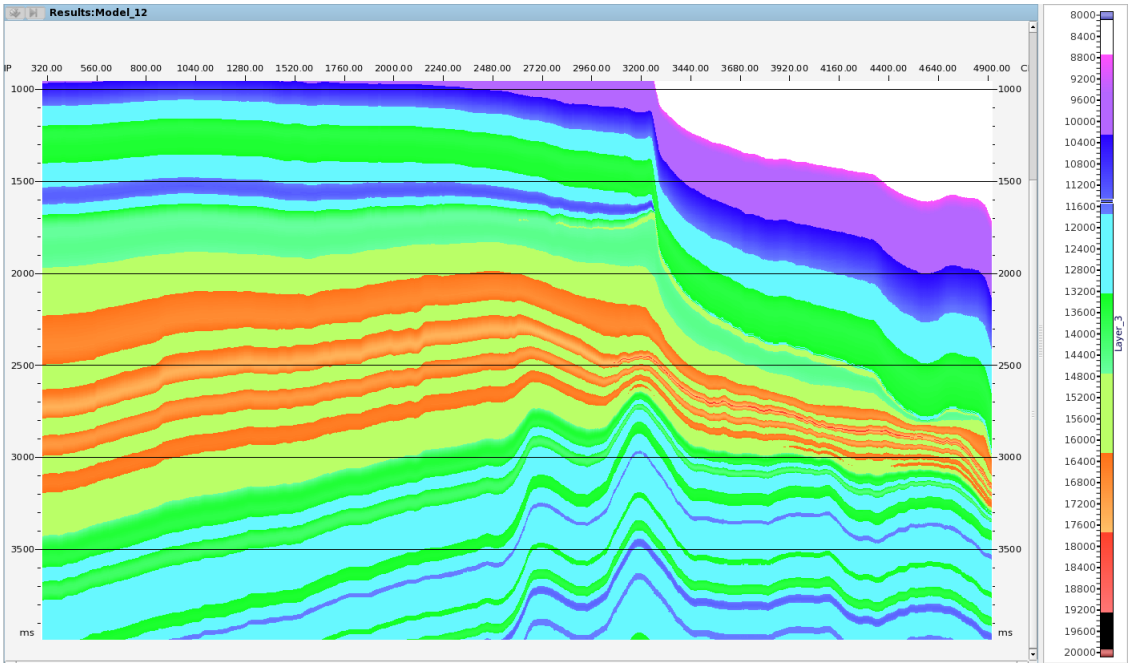

Figure 11. Initial model of the Inversion.

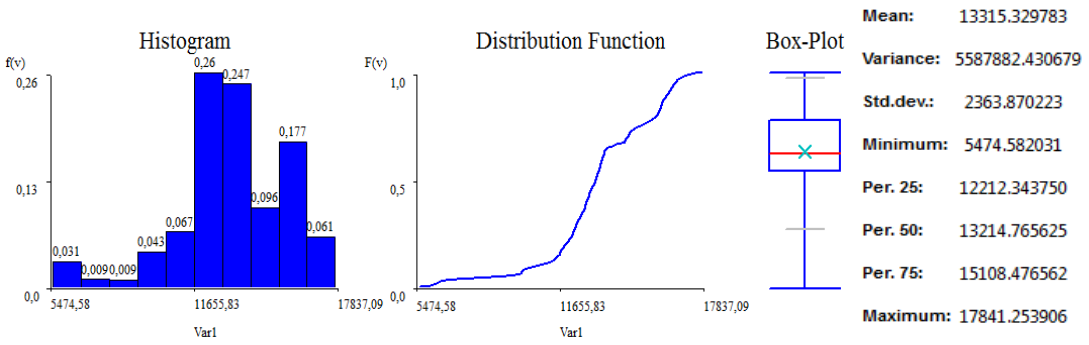

Figure 12. Data analysis for the initial model of the Inversion

According to the data analysis performed in the initial model (figure 12), this has values of impedance between 5474 (m/s)*(g/cc) and 17837 (m/s)*(g/cc) and its mean value is 13315 (m/s)*(g/cc).

Once the initial model is created it is possible to run the inversion, where it is necessary to introduce some parameters:

- Model constraint option. In this parameter is set the percentage of constraint of the final result to the initial model. In this case a value of 0.5 was introduced, having therefore a contribution of 50 percent of each element (seismic and initial model).
- Average block size: This parameter sets the thickness in milliseconds layers in travel time of the model. In this case a value of 4 ms was chosen, which represents the sample rate of the seismic.
- Prewhitening. This parameter determines the noise level that is added to the amplitude spectrum of the data before the analysis. Is recommended to leave this parameter in default (1%) and only modify it if a problem with the convergence of the inversion is found.
- Number of iterations. In this case 25 iterations were used.
- Scaler option. This process estimates a scale factor assuming a known average reflection coefficient size and matching the derived reflectivity from the seismic to that value. The software gives two options, to perform the calculation of a single global scaler or separate scalers for each trace. In this case the first option was used, in which a scaler value is calculated in a window of traces and then is applied to all the data.

The final result obtained in this inversion is going to be shown in the chapter 5.

4.2 Global Stochastic Inversion

The Global Stochastic Inversion was performed using a computational code which is currently being developed in the CERENA at the Instituto Superior Tecnico. It is important to mention that this inversion is more flexible than the Model-based inversion, because it has as advantage that it does not need log data in the survey and it is possible to use logs from other places in the area a similar geology and making use of this technique suitable for under-sampled reservoirs. In this case was used the wavelet shown before, but a new pseudo-log for acoustic impedance was used, which was generated by extracting a trace from the result of the model-based inversion, in order to have a new pseudo-log with the contribution of the seismic. Figure 13 shows the pseudo-log of P-impedance used in the inversion processes.

The minimum and maximum values of the property and the parameters of the modeled variograms are required as inputs in the execution of the program, for that reason the exploratory data analysis and the spatial data analysis were performed.

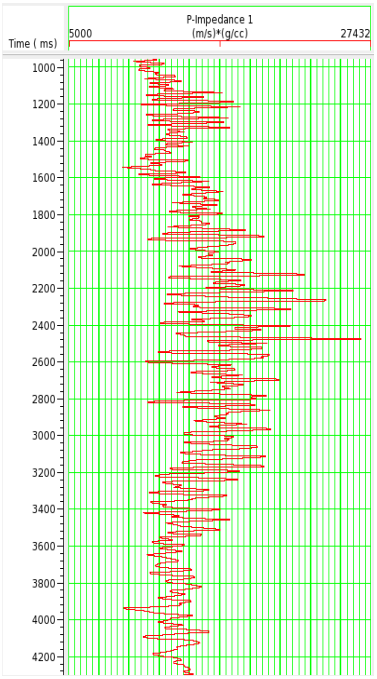

Figure 13. Pseudo-wells of P-impedance used for the Global Stochastic Inversion.

4.2.1 Exploratory data analysis

The exploratory data analysis is implemented with the objective of characterizing the statistical behavior of the data. In this step are performed histograms and obtained values, for example the mean, variance and standard deviation. This analysis was performed for the pseudo-well. In the next figure is shown the histogram, the distribution function and box-plot obtained.

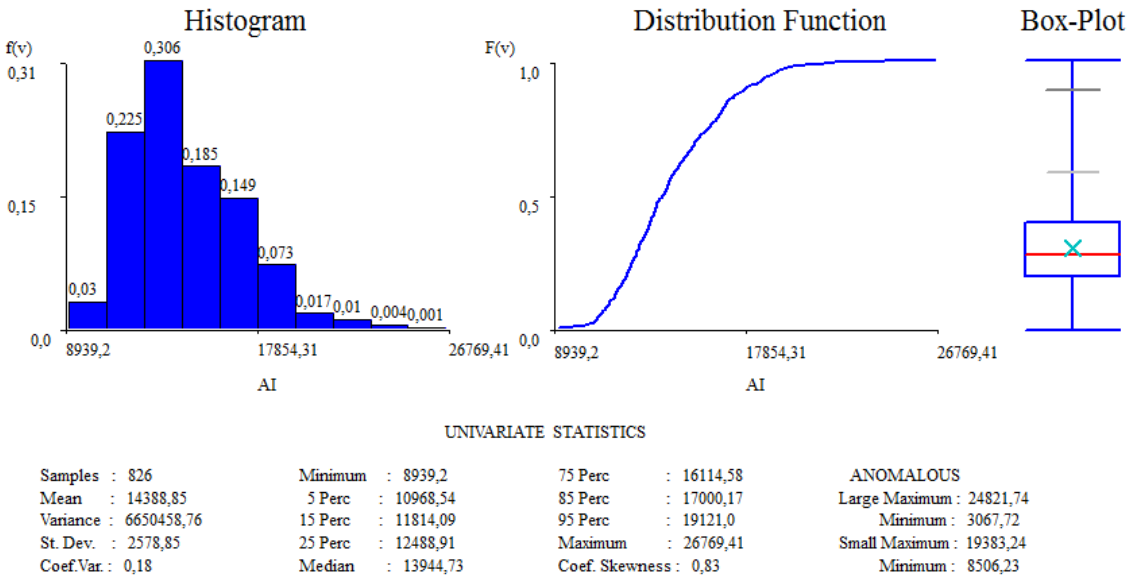

Figure 14. Data analysis for the pseudo-log of acoustic impedance

In the figure 14 can be observed that the well log has a range from 8932 (m/s)*(g/cc) to 26769 (m/s)*(g/cc), the mean is 14389 (m/s)*(g/cc), the median is 13944 (m/s)*(g/cc) and the variance is 6650458. The histogram is asymmetric and positive, with a coefficient of 0.83, having more frequency of occurrence of smaller values and therefore the median is smaller than the mean.

4.2.2 Spatial data analysis

The spatial data analysis is performed to establish a quantitative measure of the spatial correlation. In this stage were calculated experimental variograms, for the seismic and for the well data. After the calculation these variograms were adjusted to the theoretical models described before. Due the data limitation only two directions were considered, the vertical direction with azimuth= 0º and dip=90º and the horizontal direction with azimuth =90º and dip= 0º. The variogram in the vertical direction was calculated from the well data and the variogram in the horizontal direction from the seismic data. It is important to point that in the case of the vertical variogram the lag distance was 4, corresponding to the sampling rate of the log extracted from the model-based inversion (4 ms). For the horizontal variogram the lag distance is 12.5 m, which is the distance between two contiguous CDPs. The parameters used to model the variograms are in the table 1.

Table 1. Parameters used in the variogram modeling for the input data

Angle	Horizontal range	Sill
(0,90)	22 ms	4759085
(90,0)	1250 m	32

The variograms calculated and the adjustment to a theoretical model are shown in the figures 15 and 16.

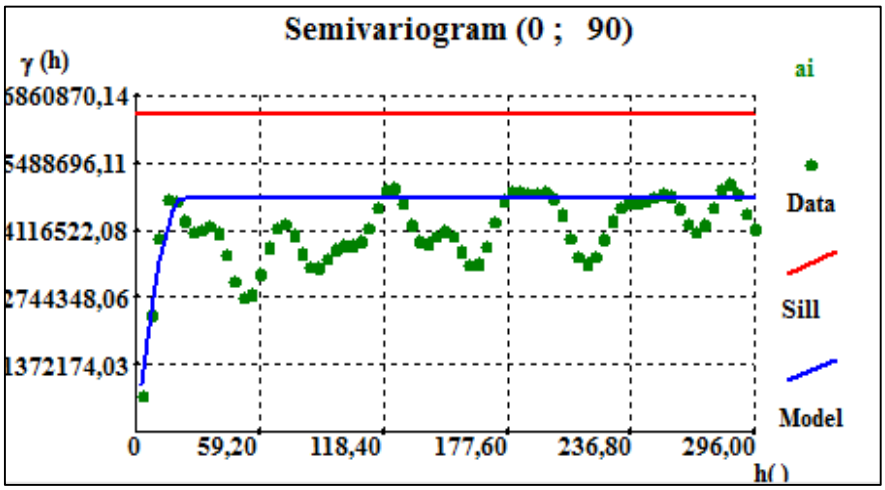

Figure 15. Vertical variogram (Green filled circles) and modeled variograms (blue line) for the input data.

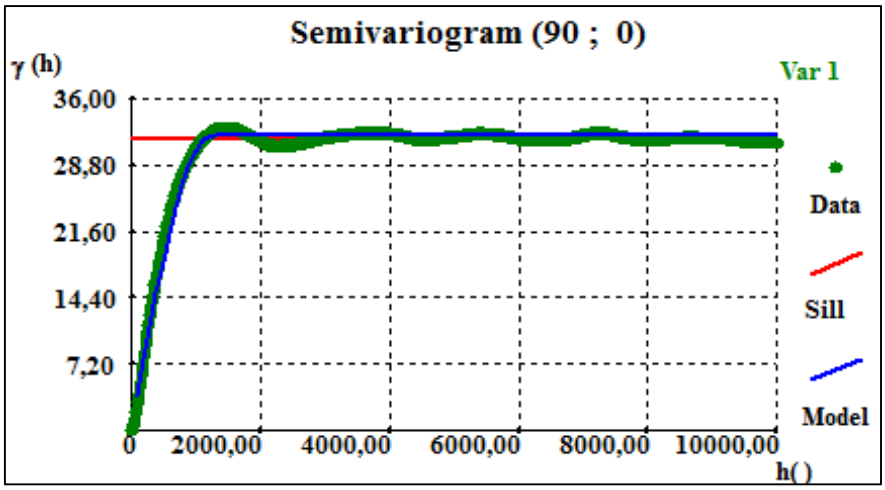

Figure 16. Horizontal variogram (Green filled circles) and modeled variograms (blue line) for input data.

In both cases the adjustment was performed with a spherical model, which is commonly encountered in the model in geostatistics. For the vertical variogram it is possible to observe a cyclical behavior in the variogram that could be related with variations in the lithology in the vertical axis, which in this case is in milliseconds.

4.2.3 Execution of the GSI

After the geostatistical data analysis was performed, Global Stochastic Inversion executed with different approaches which are going to be explained below. One of the advantages of the GSI is the possibility to work without well data located inside the study area, for this reason the well was relocated outside the area. Is important to mention that in all the inversions 6 iterations were performed with 32 simulations in each iteration.

4.2.3.1 Using the input used in the Model-based Inversion

In this case the soft-model of the inversion is the input used in the model-based inversion. In the inversion in the simulation stage is considered a direct sequential simulation using a simple kriging with local means, where the local means are set by the input image.

4.2.3.2 Using a model divided by zones according to the geological interpretation

For this case it is necessary to build a model indicating zones based on the geology of the area, the main idea is to group layers with a similar behavior in the properties. Figure 17 shows the model of zones used in the GSI.

It is important to mention the well should be divided taking into account the zones and for each one must be input the maximum and minimum values of the property in the range. The histograms for each zone are shown in figure 17.

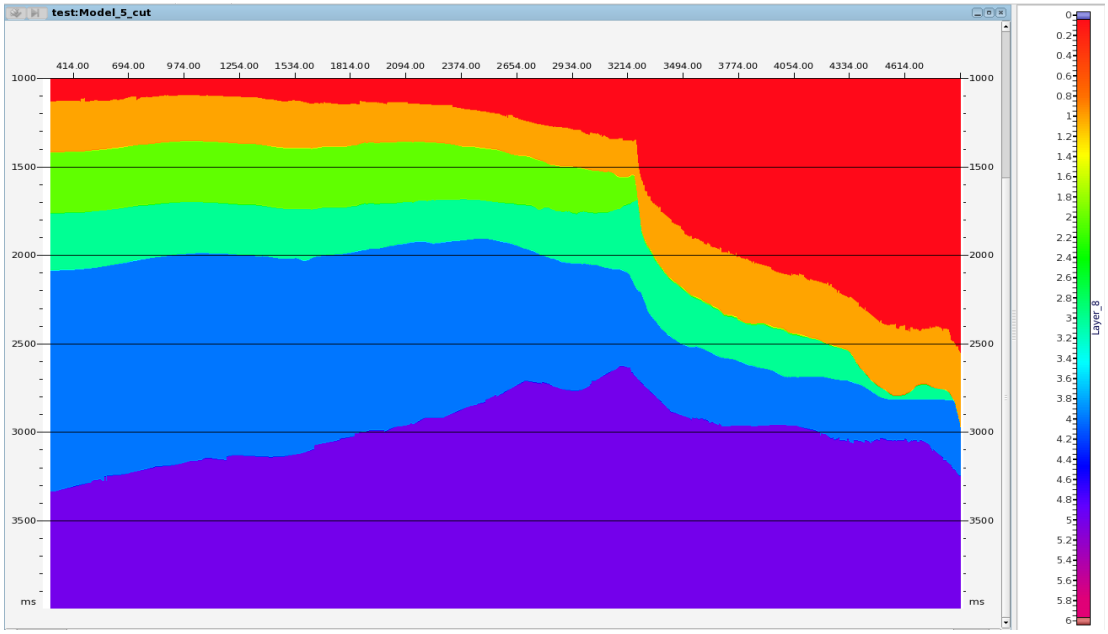

Figure 17. Model of zones used as input in the GSI.

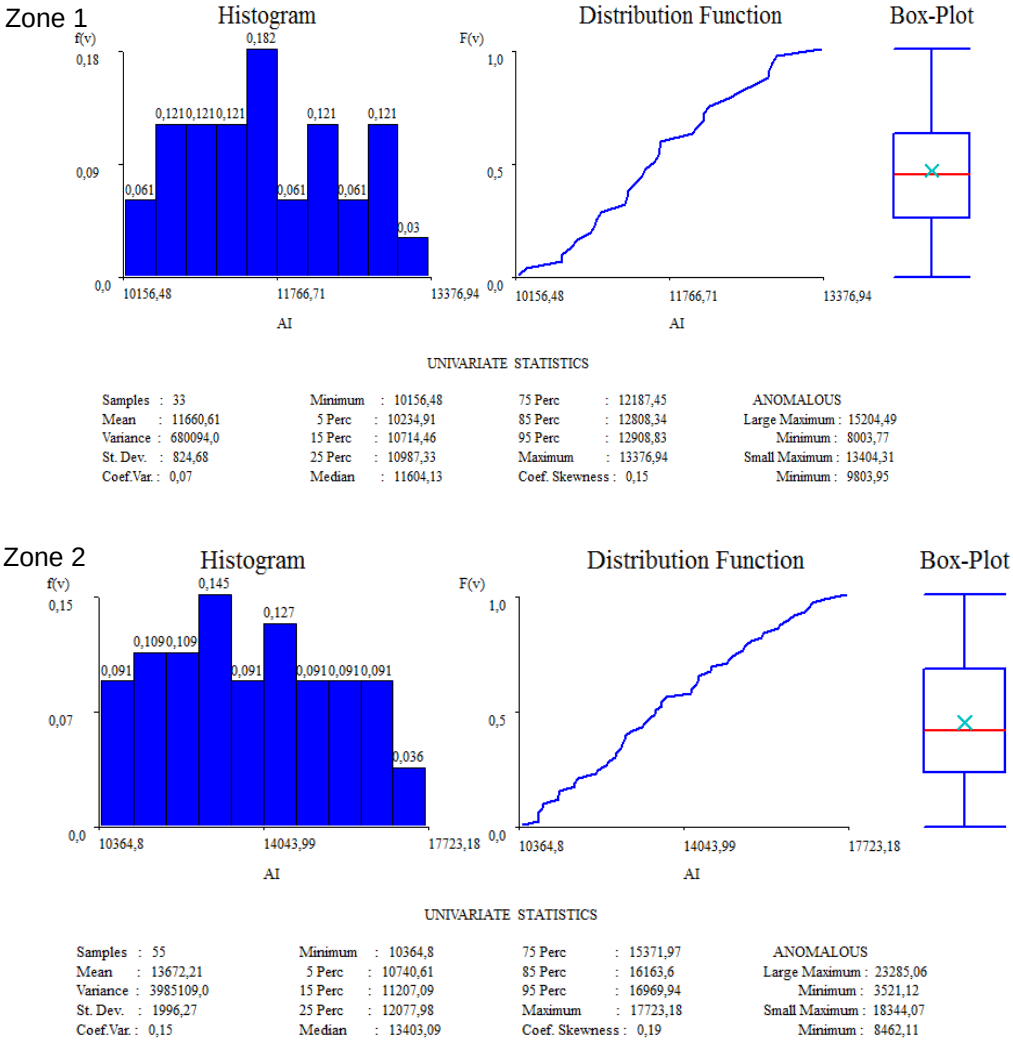

Figure 18. Data analysis for the pseudo-log of acoustic impedance in each zone.

Zone 3

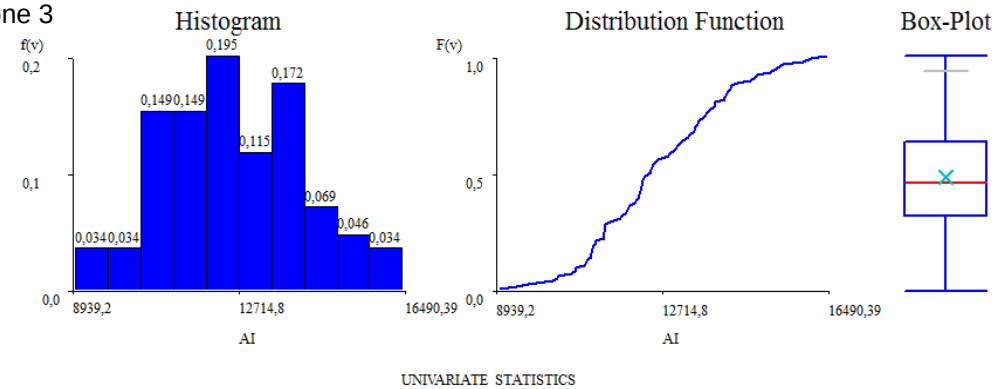

UNIVARIATE STATISTICS

Samples	87	Minimum	8939,2	75 Perc	13747,85	ANOMALOUS	
Mean	12607,97	5 Perc	10265,13	85 Perc	14208,61	Large Maximum	19580,99
Variance	2524119,0	15 Perc	11069,84	95 Perc	15401,38	Minimum	5282,45
St. Dev.	1588,75	25 Perc	11364,76	Maximum	16490,39	Small Maximum	16006,35
Coef.Var.	0,13	Median	12431,72	Coef. Skewness	0,21	Minimum	8857,08

Zone 4

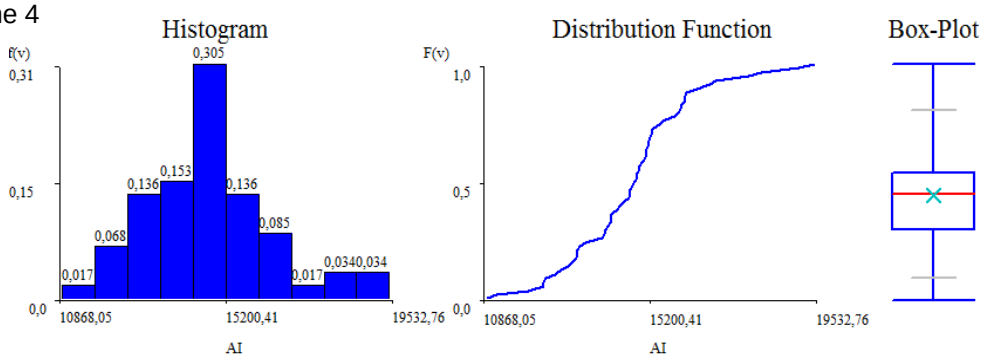

UNIVARIATE STATISTICS

Samples	59	Minimum	10868,05	75 Perc	15536,99	ANOMALOUS	
Mean	14715,64	5 Perc	11957,88	85 Perc	16127,65	Large Maximum	20946,92
Variance	2865322,0	15 Perc	13021,56	95 Perc	18142,28	Minimum	8618,96
St. Dev.	1692,73	25 Perc	13482,33	Maximum	19532,76	Small Maximum	17864,93
Coef.Var.	0,12	Median	14782,94	Coef. Skewness	0,38	Minimum	11700,95

Zone 5

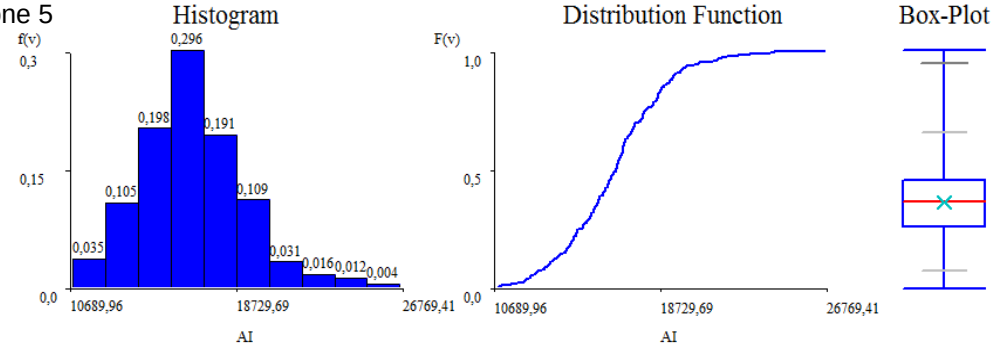

UNIVARIATE STATISTICS

Samples	257	Minimum	10689,96	75 Perc	17970,72	ANOMALOUS	
Mean	16520,71	5 Perc	12342,67	85 Perc	18895,53	Large Maximum	25851,14
Variance	6564296,27	15 Perc	14041,13	95 Perc	21235,3	Minimum	7199,9
St. Dev.	2562,09	25 Perc	14862,18	Maximum	26769,41	Small Maximum	21188,33
Coef.Var.	0,16	Median	16525,52	Coef. Skewness	0,49	Minimum	11862,71

Figure 18. Data analysis for the pseudo-log of acoustic impedance in each zone (continuation).

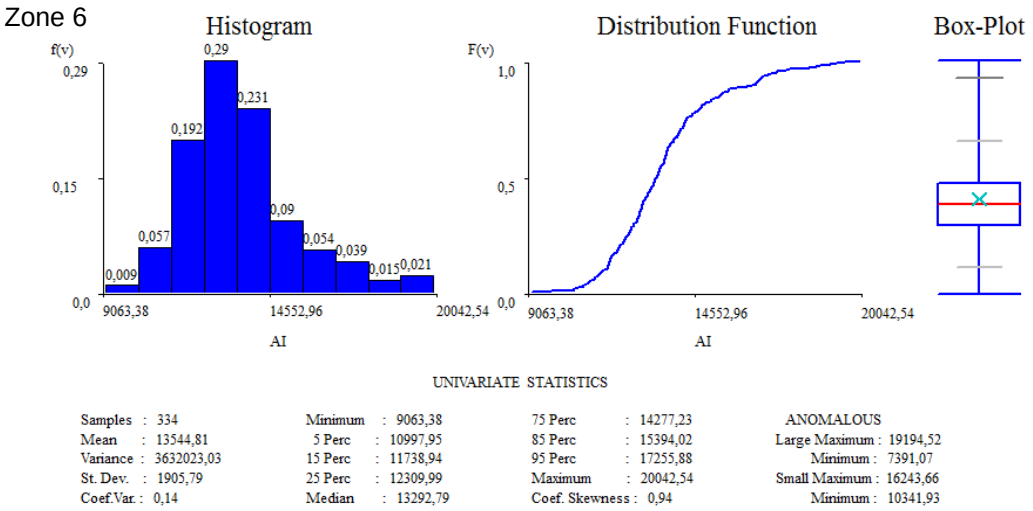

Figure 18. Data analysis for the pseudo-log of acoustic impedance in each zone **(continuation).**

In this case the simulations are performed with a direct sequential simulation, using a simple kriging with local means, where the local means are set by the local histograms. The input for the simulations of the first iteration the same initial soft-model used in the model-based inversion (figure 11).

4.2.3.3 Using the output from the deterministic inversion

The input for this inversion was the result obtained in the deterministic inversion. The simulations and the co-simulations are performed using a direct sequential simulation with a simple kriging with local means for the first iteration and after the first iteration using a collocated co-kriging with local means, where the best section is used as secondary variable and the result obtained in the deterministic approach is used as image of local means The idea to use the deterministic inversion as input is to refine the result obtained in the model-based inversion.

5. RESULTS

5.1 Model-based Inversion.

Figure 19 shows the result obtained in the model-based inversion, where is evident that exists a correspondence in the trend of the values of acoustic impedance compared with the initial model (figure 11). In this result is also obvious the influence of the seismic, reproducing inclusive the noise present in it, which is expecting because this type of inversion tries to match the inverted model and the seismic events in places even with a low signal-noise ratio. This could be mitigate with more constrain to the input low-frequency model, but in this case taking into consideration that this model was generated only with one pseudo-well, was decided to have an equal contribution of the model and the seismic.

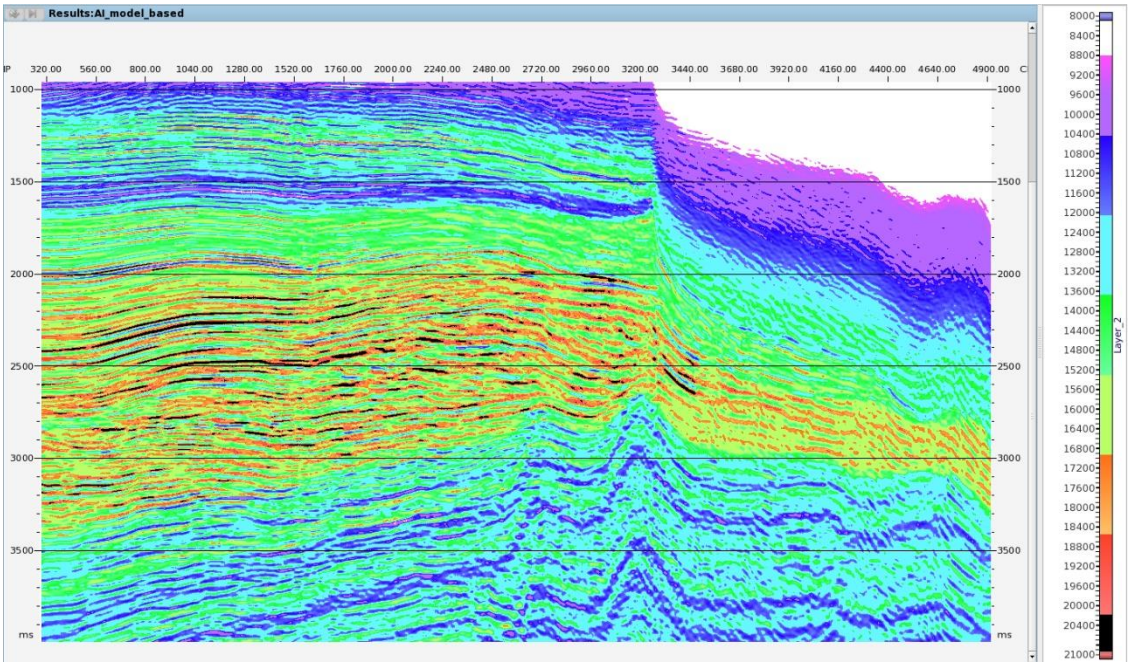

Figure 19. Model-based inversion result

The statistics shows that inverted section of acoustic impedance has values between 5152 and 27331 (m/s)*(g/cc)with a mean value of 13373 (m/s)*(g/cc)and the variance of 7428455

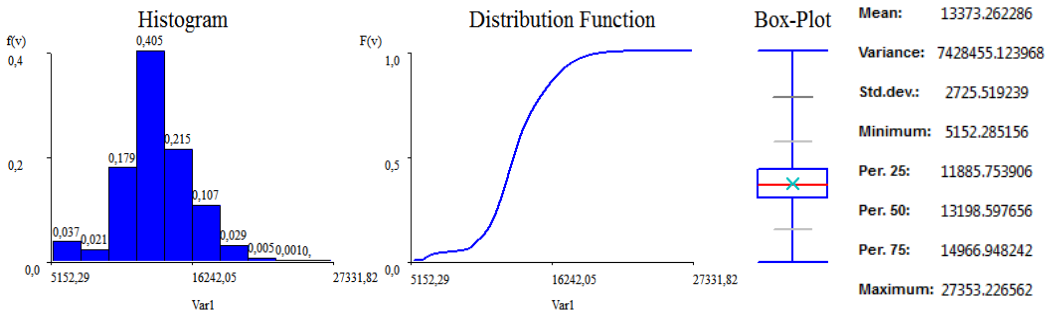

Figure 20. Histogram and statistics of the model-based inversion result

Figure 21 shows the synthetic seismic data generated in the model-based inversion, which is very similar to the input seismic data shown in the past section (figure 7), this was expected considering the high contribution of the seismic data in the inversion result, which is evident in figure 19. The error of the model-based inversion was calculated by the difference between the input seismic data and the synthetic calculated in the inversion and is in figure 22, where is possible to observe in general is very low, even in zones where the data signal-noise ratio is poor, which means that the inversion result is not only reproducing the seismic behavior, it is also reproducing the noise present in the seismic data.

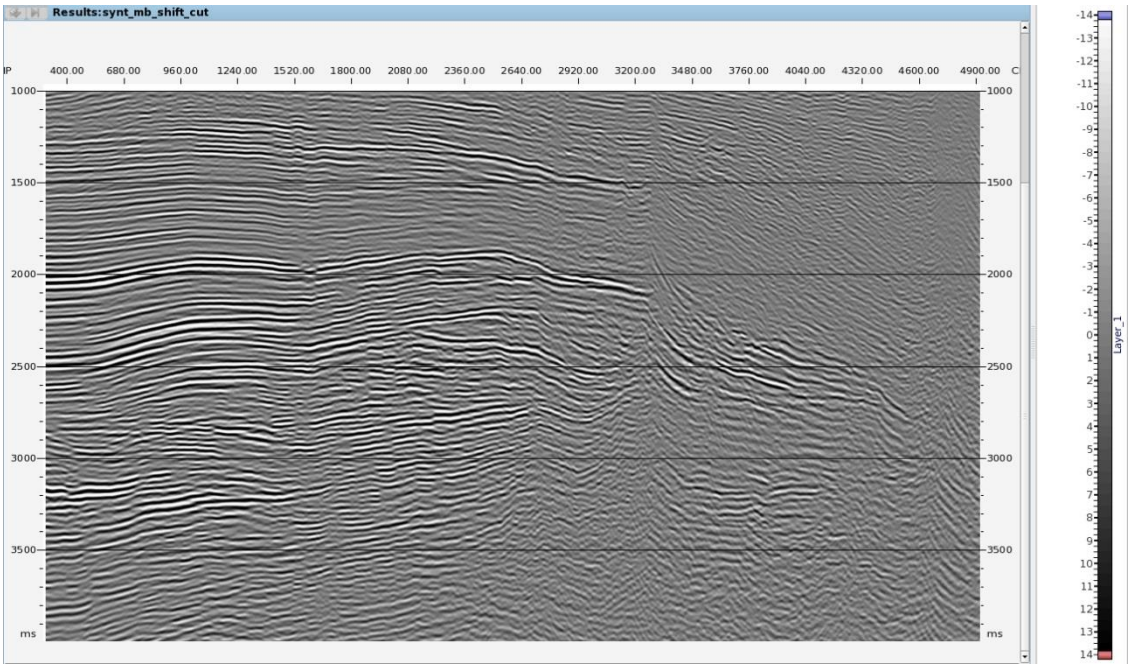

Figure 21. Model-based inversion synthetic

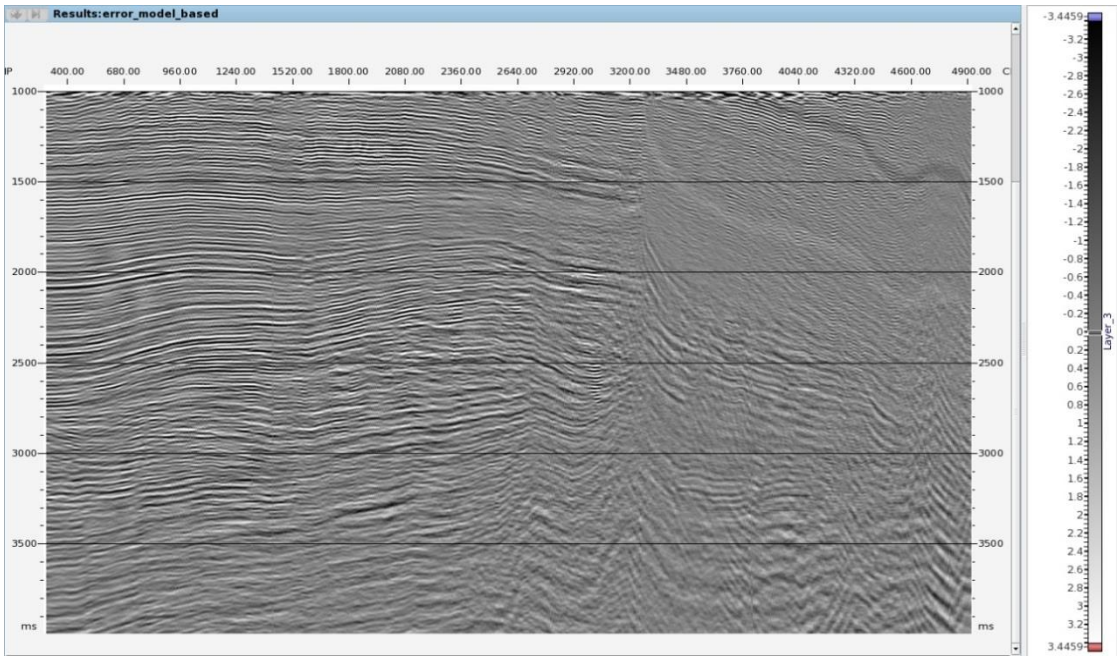

Figure 22. Error associated with the model-based inversion

5.2 Global Stochastic Inversion

5.2.1 Case1: GSI with the input used in the Model- based Inversion as local trend

The result obtained in the GSI using as input the input model used in the deterministic approach (figure 11) could be observed in figure 23:

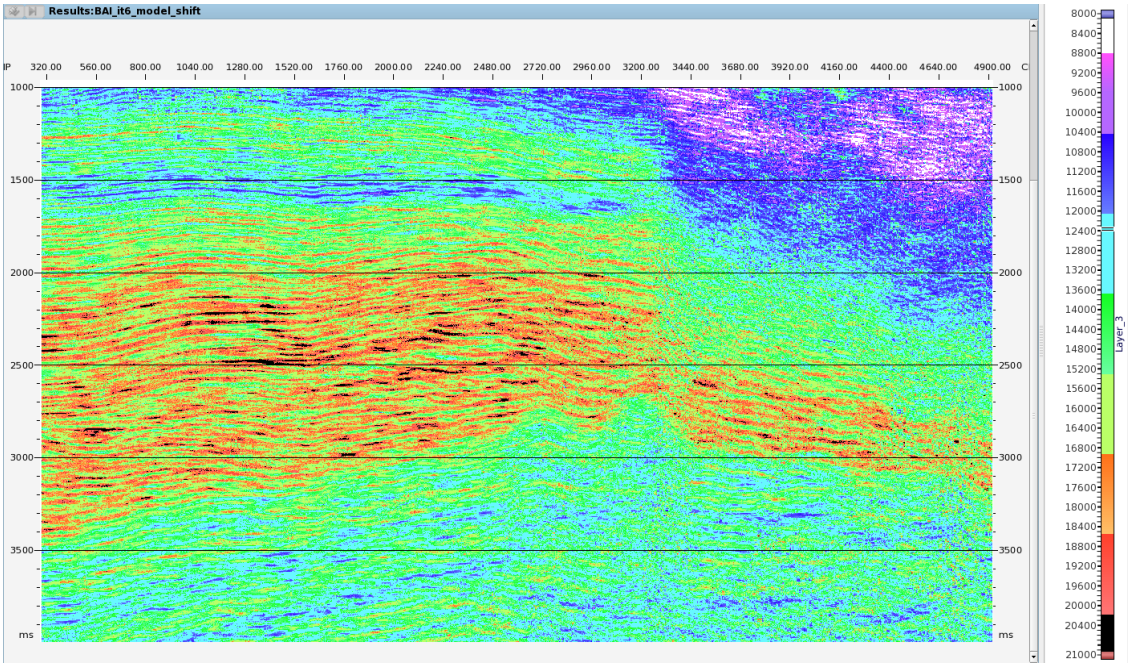

Figure 23. Best acoustic impedance section obtained in case 1.

In the previous figure, could be observed that the result has a seismic behavior, but with a better attenuation of the noise compared to the result obtained for the model- based inversion. It is also evident that the inversion result has a correspondence with the input model, and therefore the model is being respected, nevertheless this correspondence is less evident than in the result obtained for the model based inversion.

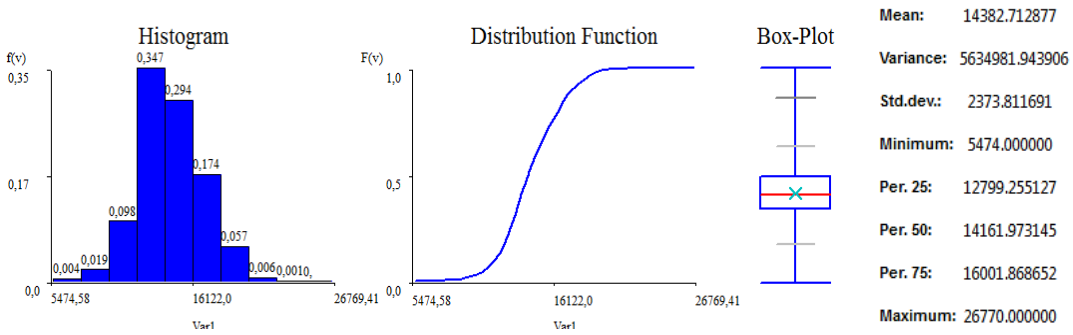

Figure 24. Histogram and statistics of case 1.

As it was mentioned in the pass section, in the execution of the GSI, it is possible to set the minimum and maximum values allowed in the output of the inversion process. In this case the minimum values was conditioned by the minimum value of the well (5474(m/s)* (g/cc,) and the maximum value by the input model (26769 (m/s)*(g/cc)). To condition these values is necessary in order that the algorithm works properly and it is also justified by the fact that only one well is used in the inversion, which does not necessary represent the behavior of the property in entire area. It is expected that histogram of the well do not be honored, because there is an important difference between the minimum values between the result and the pseudo-log data (8932 (m/s)*(g/cc)).

The GIS has the capability to calculate and reproduce as outputs the synthetic seismic sections calculated in each simulation. Figure 25 shows the synthetic obtained for one simulation of the last iteration, in which is possible to observe that the main structure is reproduced and in some areas (between 1.5 and 2 seconds) the reflectors have been enhanced. In areas where the signal-noise ratio is low (between 1 and 1.5 second and CDP's 3800-4900) the synthetic has information, nevertheless is not coherent and has not correlation with the input data (figure 7). It is also evident that there is a difference in the relative amplitudes between the reflectors compared to the input data, which was not observed in the synthetic calculated in the model-based inversion, in which the software as part of the inversion procedure applies a scaling to the amplitude of the synthetic.

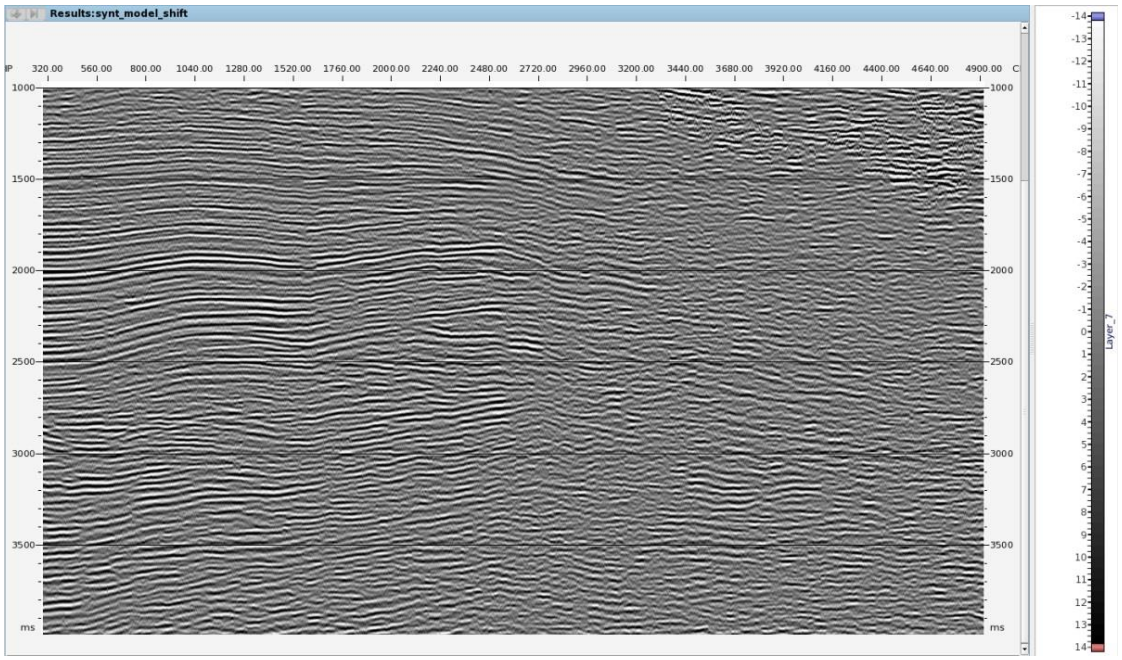

Figure 25. Synthetic calculated in case 1.

Table 2. Parameters used in the variogram modeling for the result of case 1.

Angle	Amplitude	Sill
(0,90)	22 ms	3119375
(90,0)	1250 m	39

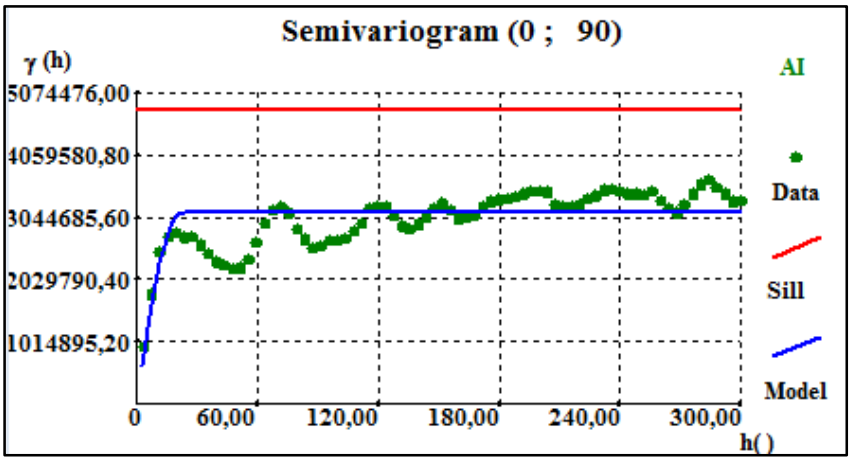

Figure 26. Vertical variogram (Green filled circles) and modeled variograms (blue line) calculated for the result of case 1.

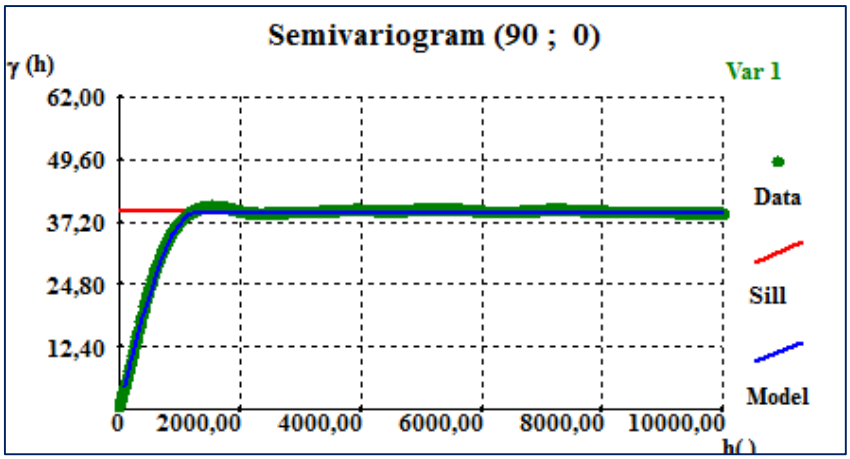

Figure 27. Horizontal variogram (Green filled circles) and modeled variograms (blue line) calculated for the result of case 1.

Another characteristic of GSI is the reproduction of spatial continuity pattern of acoustic impedance as they are revealed by the variogram. As a quality control of the result, the horizontal and vertical variograms were calculated. The vertical variogram (figure 26) was calculated extracting a trace of the best acoustic impedance section and the horizontal variogram was calculated from the synthetic shown before (figure 27). The parameters used to model the variograms are shown in table 2. For both variogram were obtained the same values of the amplitude shown in the past chapter for the well log data (figure 15) and the input seismic (figure 16), which means that the spatial continuity of the variable is reproduced. The maximum variance for both variogram is different that the values shown before. For the vertical variogram, it is also possibly to observe a cyclic behavior, similar to that observed in the variogram performed for the well log data.

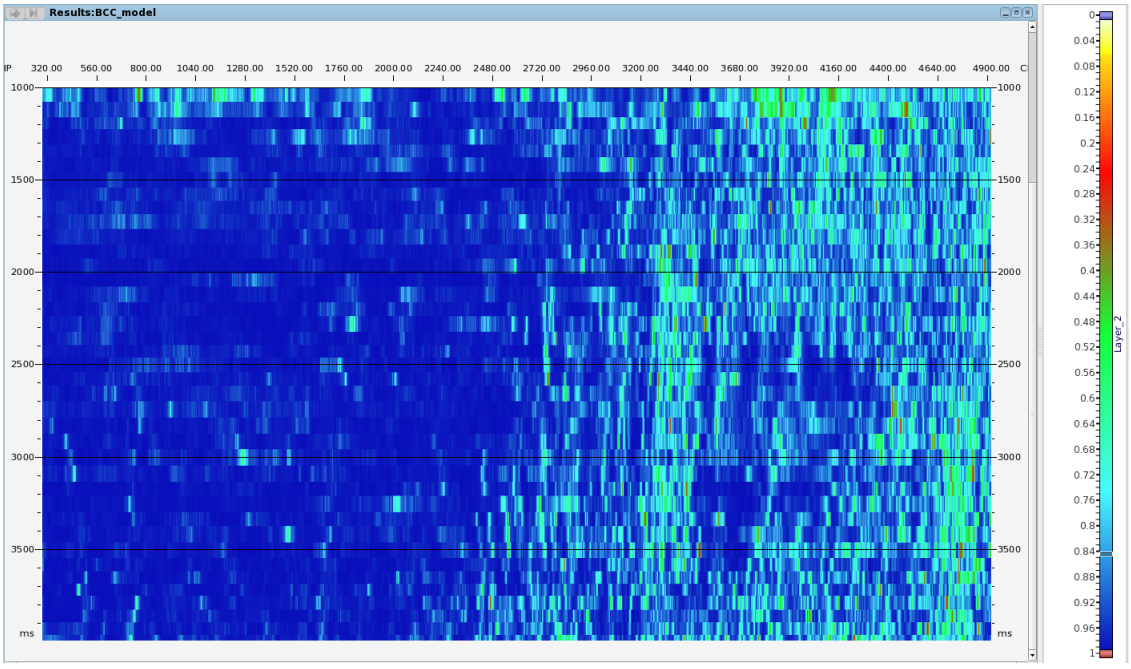

Figure 28. Best correlation section for case 1.

Figure 28 is the best correlation section obtained in the iteration number 6 and figure 28 represents the histogram and statistics calculated for this, which is possible to observe that in general the results show a high correlation, with a mean value is 0.91, a minimum of 0.14 and a maximum of 0.99. The low values in the correlation are in zones where the seismic input data has low quality and the synthetic shown before (figure 25) has a bad definition of seismic events.

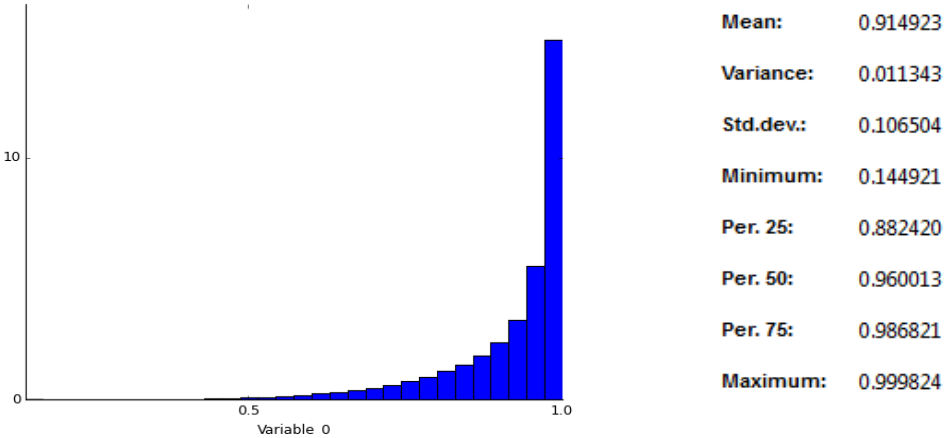

Figure 29. Histogram and statistics of the best correlation section for case 1

The mean value of the simulations for the last iteration could be observed in figure 30, which compared with the best section (figure 23), looks smoother and has less definition of the events in places where the signal-noise ratio is higher, which means that the inversion procedure is being responsible for the definition of the events in those areas and also gives the seismic behavior to the final result.

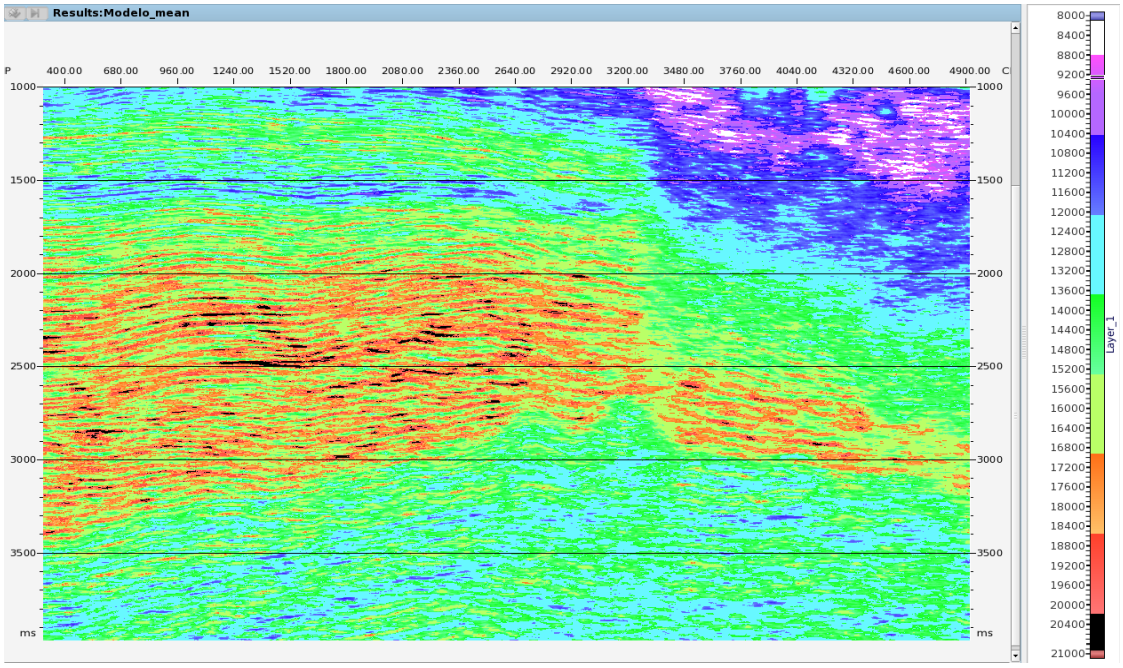

Figure 30. Mean calculated for case 1.

Next figure shows the histogram calculated for the mean of the simulations, which compared with the histogram shown for the results obtained in the GSI (figure 24), has a similar shape, similar values for the mean, but has a significant difference in the variance (774920), being lower the variance calculated for the mean of the simulations, which is expected because this result is smoother than the result obtained in the GSI and therefore there is less variability in the data. The mean of the simulations overestimates the minimum value (5925 (m/s)*(g/cc)) and underestimates the maximum value (26769 (m/s)*(g/cc)), compared with those imposed to the inversion.

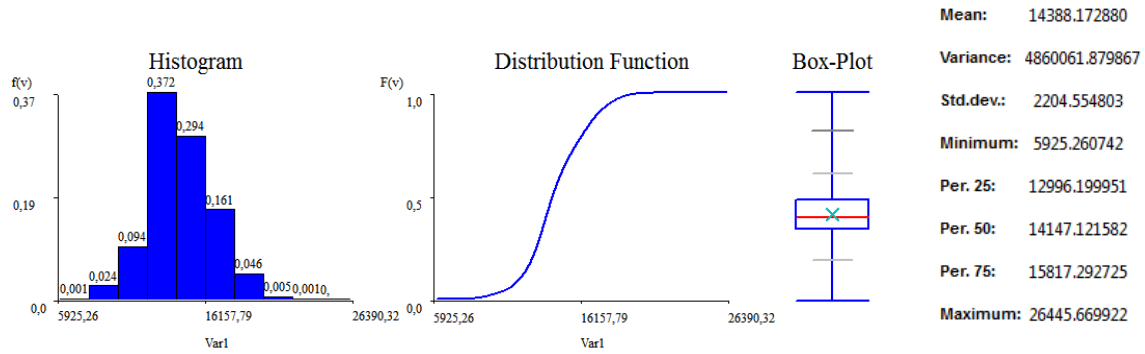

Figure 31. Histogram and statistics of the mean calculated for case 1

The variance for all the simulations of the last iteration was calculated and is shown in figure 32, where it is possible to observe that the variance has the highest values (blue zones in figure 32) in zones where the seismic quality is poor, being related with those areas where the synthetic has problem in the definition of the seismic events.

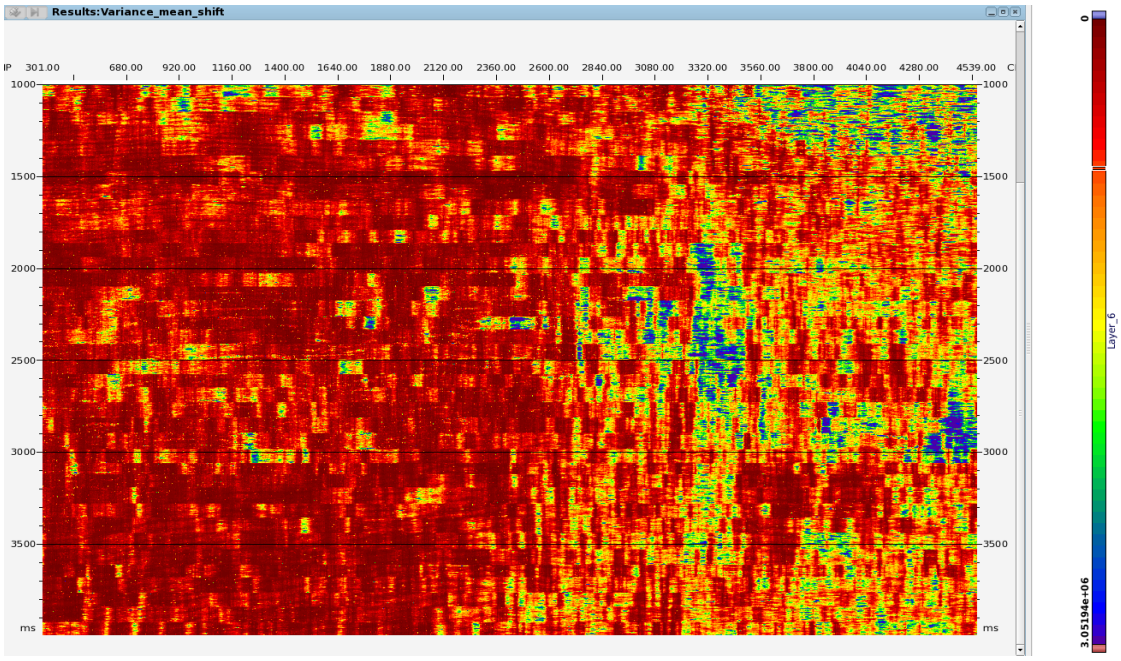

Figure 32. Variance calculated for case 1.

5.2.2. Case 2: Using a model divided by zones according to the geological interpretation.

The study area was divided in 6 zones identified in figure 33, which also shows the result obtained after to execute the GSI with the initial model shown in the past section (figure 11) and dividing the section according the geological interpretation (figure 17). Due to the lateral changes in the property was hard to estimate values in some areas as for example from CDP's 3400-4900, for example the zone 0 in the result looks homogeneous and it is not possible to distinguish the changes observed in the results shown before for the deterministic approach (figure 19) and the case 1 (figure 23).

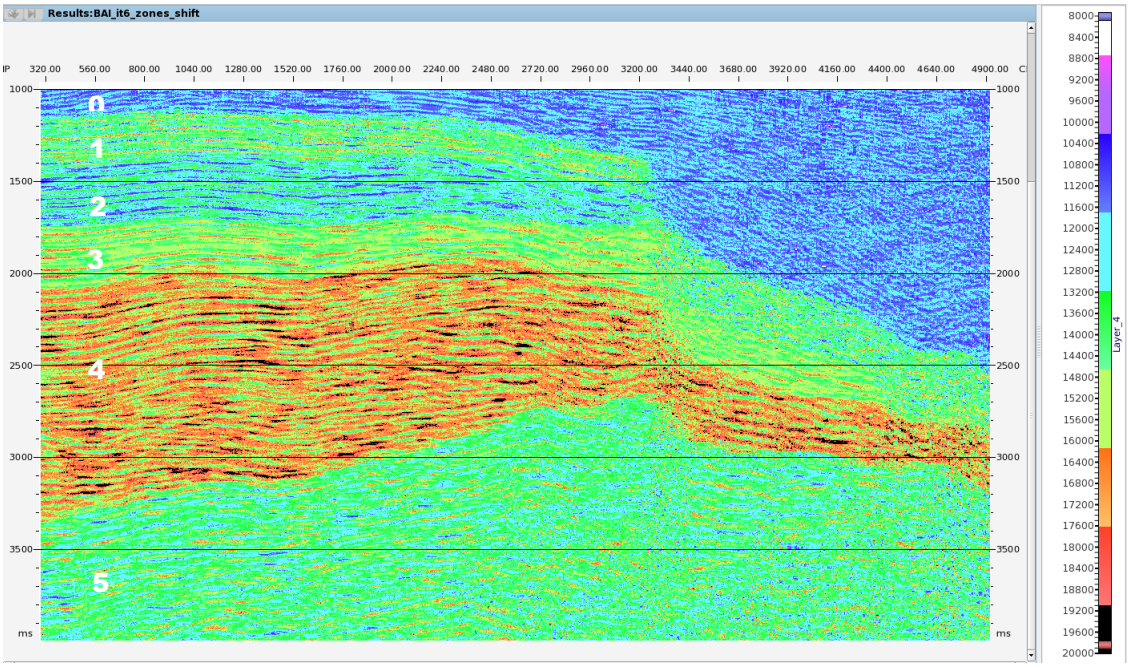

Figure 33. Best acoustic impedance section obtained in case 2

Figure 34 shows the histogram calculated for this case, where it is possible to observe that in this case the minimum and maximum values are the same observed for the case 1, the mean value in this case is 13900 (m/s)*(g/cc) and the calculated variance is 4073634.

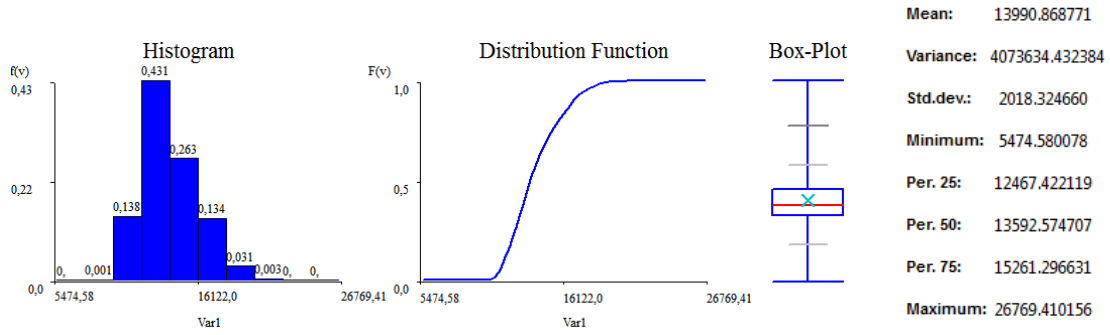

Figure 34. Histogram and statistics of case 2.

In the synthetic calculated from one simulation (figure 35), it is evident the contrast between the first two zones of the model and the lack of seismic information in the first zone. Regarding the main structure is observed the same phenomena pointed out for case 1, this has a bad definition in zones where the data has a poor quality.

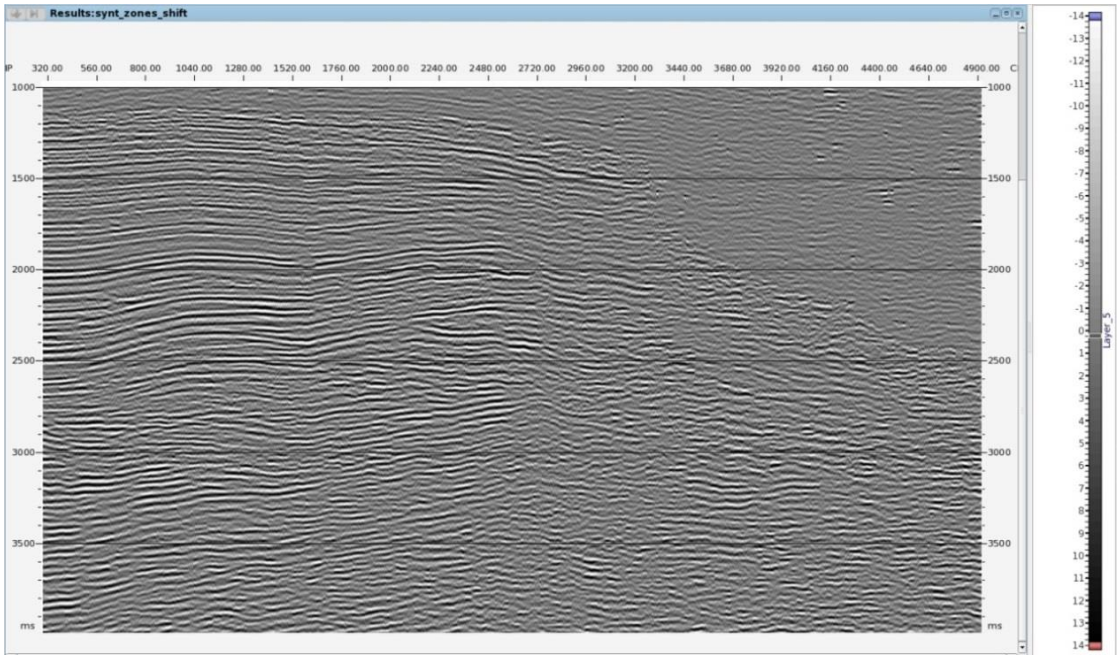

Figure 35. Synthetic calculated in case 2.

Table 3. Parameters used in the variogram modeling for the result of case 2

Angle	Amplitude	Sill
(0,90)	22 ms	2622657
(90,0)	1250 m	31

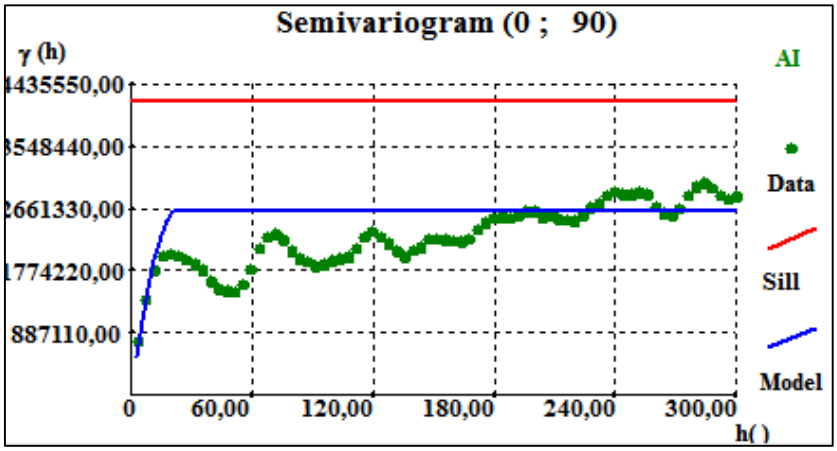

Figure 36. Vertical variogram (Green filled circles) and modeled variograms (blue line) calculated for the result of case 2.

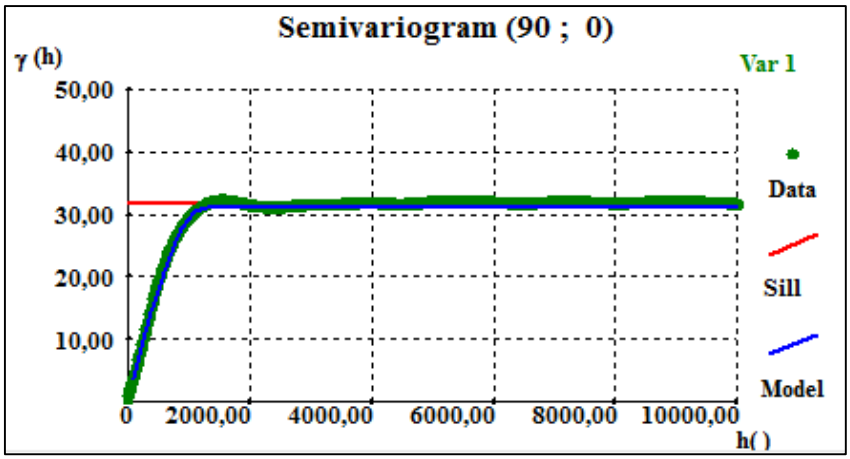

Figure 37. Horizontal variogram (Green filled circles) and modeled variograms (blue line) calculated for the result of case 2.

Table 3 shows the parameters used to model the calculated variograms (figures 36 and 37), which show the same value in the amplitude that the input variograms (figures 15 and 16), which means that the spatial continuity of the variable is being reproduced. The maximum variance for the horizontal variogram is close to the maximum variance of the seismic data, but in case of the vertical variance has an important difference. In the vertical variogram a cyclic behavior was observed.

Figure 38 shows the best correlation section obtained for this case and figure 39 the statistics calculated for it, where is possible to observe that the high correlation is 0.99, the mean correlation is 0.91, being lower in areas where the synthetic has problems to define the reflectors, which are areas where the quality of the data is poor.

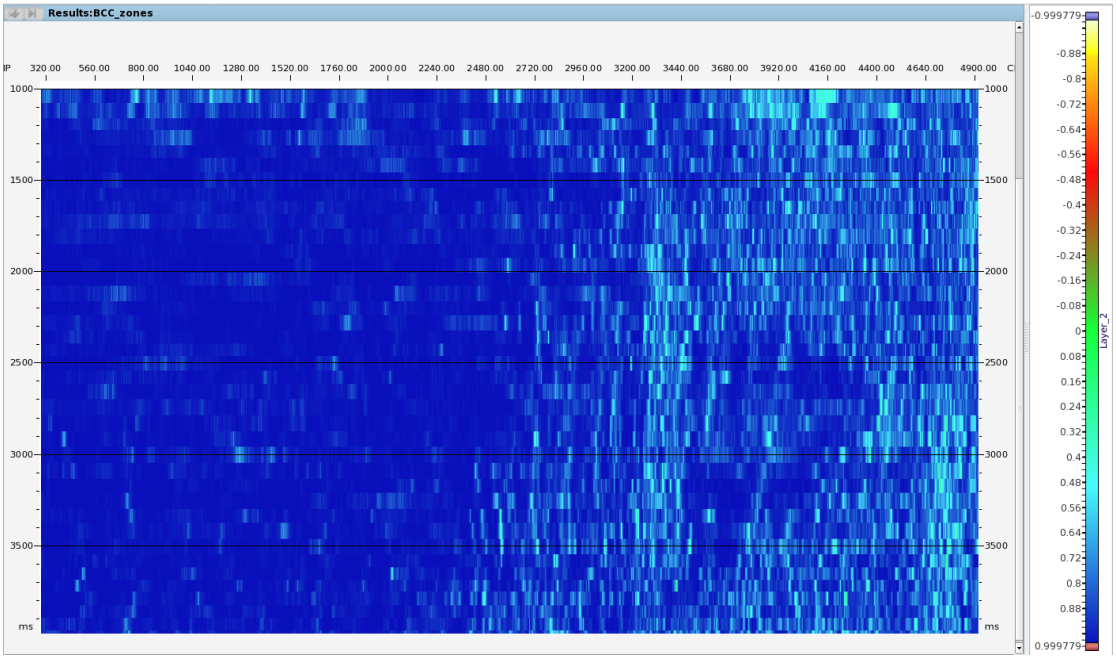

Figure 38. Best correlation section for case 2

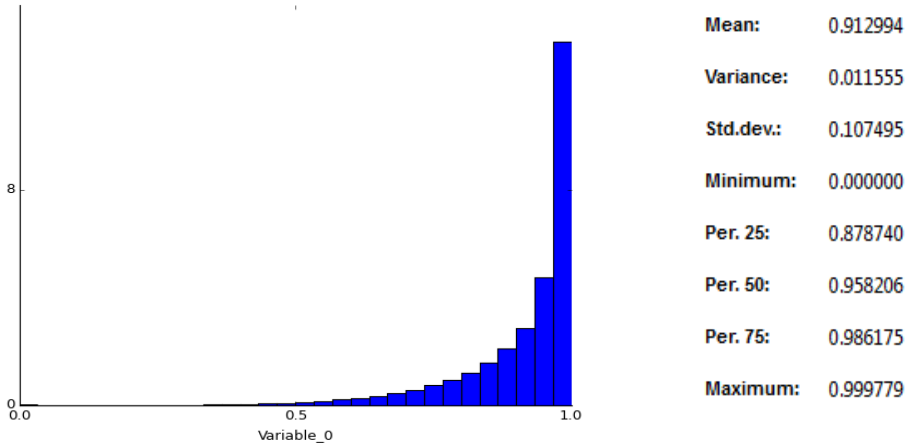

Figure 39. Histogram and statistics of the best correlation section for case 2

Figure 40 shows the mean calculated for the simulations of the last iteration, which is smoother compared to the best acoustic impedance section (figure 33). In this result the first zone (zone 0), also looks homogeneous, which is related with the difficulty to define the seismic events. This could be justified by the fact that this zone has a lateral change and the input pseudo-log is not representative of the entire zone. The histogram (figure 39) shows values between 7673 (m/s)*(g/cc) and 26011 (m/s)*(g/cc), which compared to the minimum and maximum values obtained for the best acoustic section (figure 33) are being overestimated in case of the minimum and underestimated in case of the maximum.

.

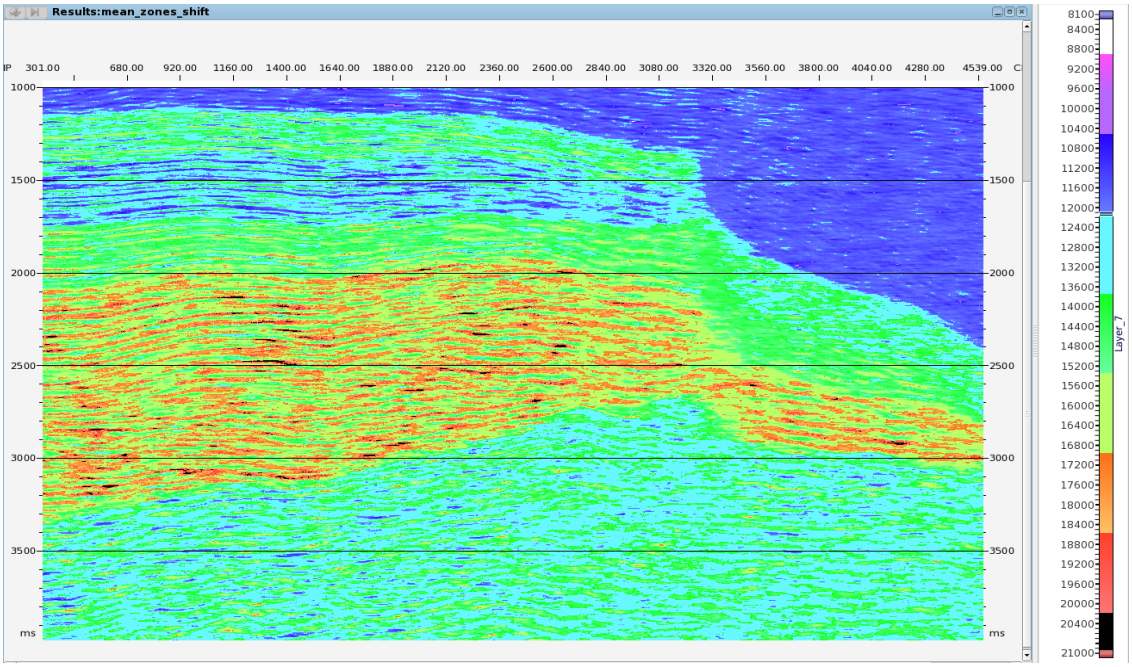

Figure 40. Mean calculated for case 2.

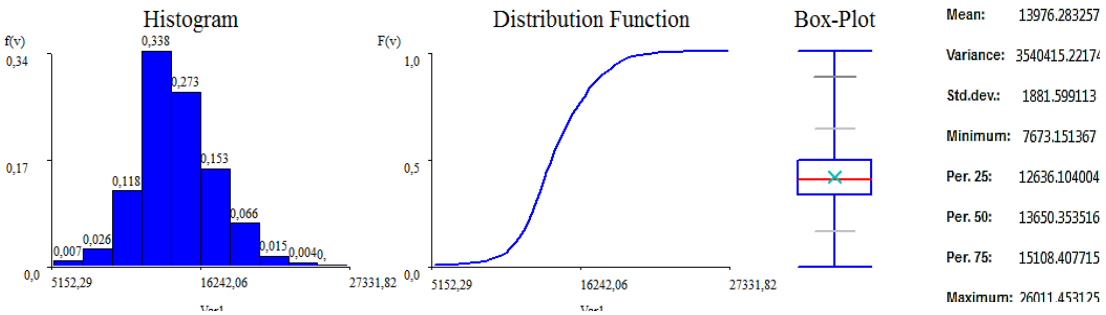

Figure 41. Histogram and statistics of the mean calculated for case 2.

In the variance (figure 42), it is evident the contrast between the zone 0 and the others zones; zone 0 has a low variance because has a low variability between the values and the minimum a maximum values of the input histogram are close. The variance is high in areas where in the synthetic did not define the seismic reflectors and where the synthetic pseudo-log has a strong difference with the values of the input model used in the inversion.

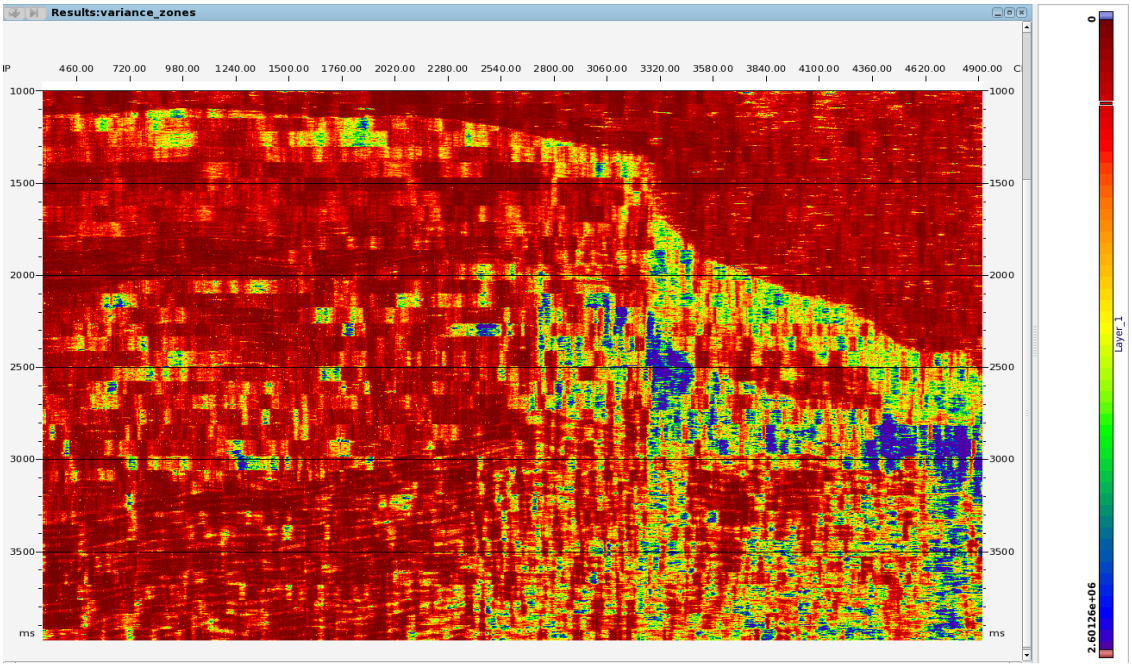

Figure 42. Variance calculated for case 2.

5.2.3 Case3: Using the output from the deterministic inversion

Figure 43 shows the result of the GSI using the output of the deterministic inversion (figure 19) as local trend. It is possible to observe that the dipping noise existing in the seismic after 3000ms is attenuated, also that the result compared with the input looks less synthetic and the initial model influence is not so strong. In this case the maximum and minimum values were fixed by the input

model, which has the entire range of values (5152 (m/s)*(g/cc) and 27331 (m/s)*(g/cc)). The histogram shows a higher value for the variance (19105987) and for the mean (14386 (m/s)*(g/cc)) compared to variance and the mean of the input model (7428455.12, 13373.26 (m/s)*(g/cc) respectively). Comparing this result with the input (figure 19), it is visible that in some events the values of the result are higher than the values of the input, nevertheless the maximum a minimum values are respected by the inversion procedure.

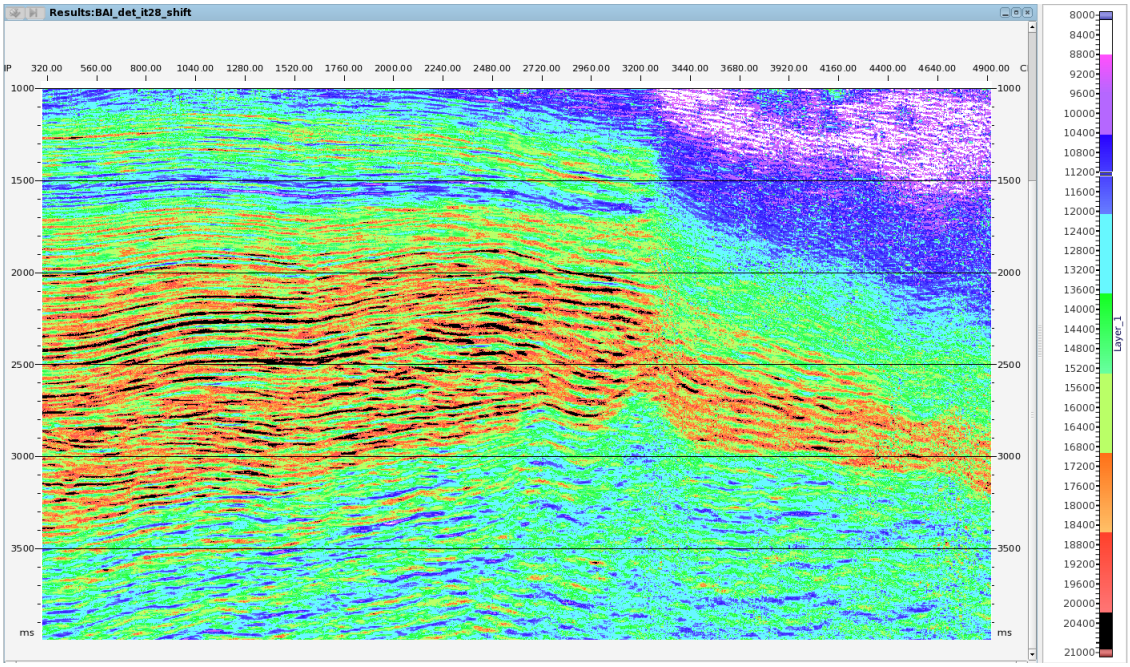

Figure 43. Best acoustic impedance section obtained in case 3

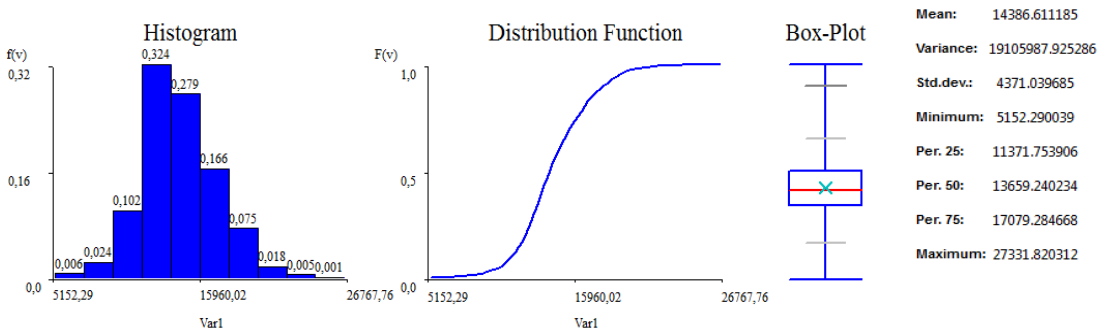

Figure 44. Histogram and statistics of case 3.

The synthetic calculated for case 3 is in figure 45, where is possible to observe that in general there is a good match with the input seismic (figure 7), with an exception in noisy areas. Comparing the synthetic calculated for this case with the synthetics calculated for case 1 and case 2, this has higher amplitudes and therefore stronger reflectors, which could be given by the fact that in this case the input has more variability and a bigger range of values.

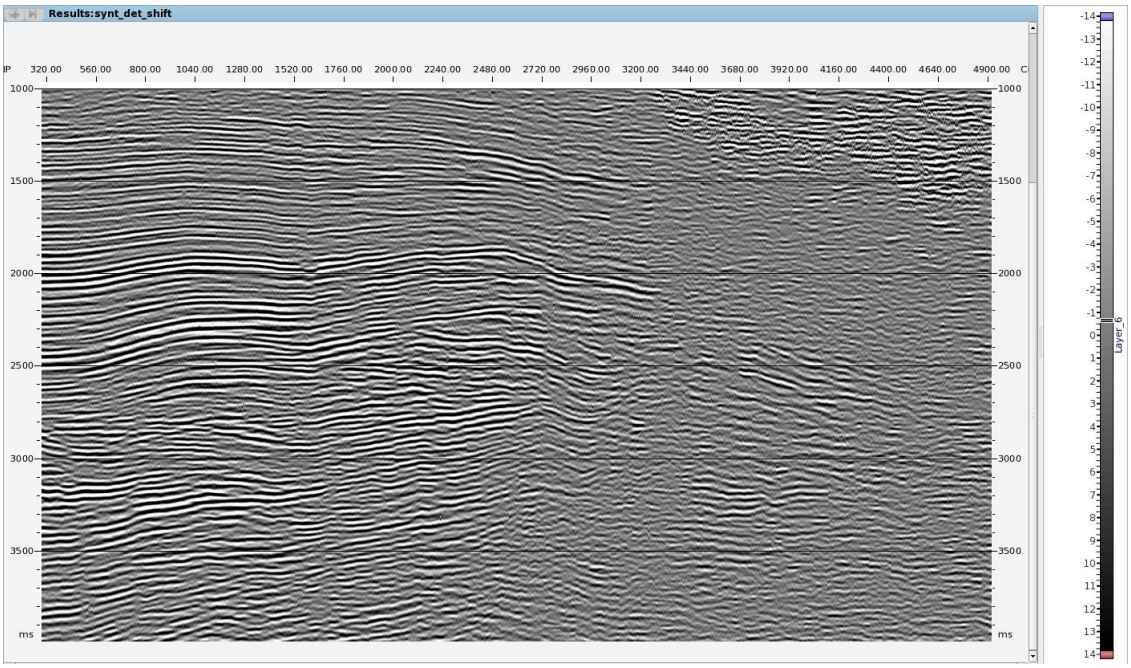

Figure 45. Synthetic calculated in case 3.

The vertical and horizontal variograms (figures 46 and 47) show the same values for the amplitudes that the variograms calculated for the well log and the input seismic data (figures 15 and 16), also the shape in both cases is similar, however, there is a variation in the sill which in both cases is higher than the sill of the input data, this could be related with the fact that the input data for this case has a high variability in both directions

Table 4. Parameters used in the variogram modeling for the result of case 3.

Angle	Amplitude	Sill
(0,90)	22 ms	5779468
(90,0)	1250 m	59

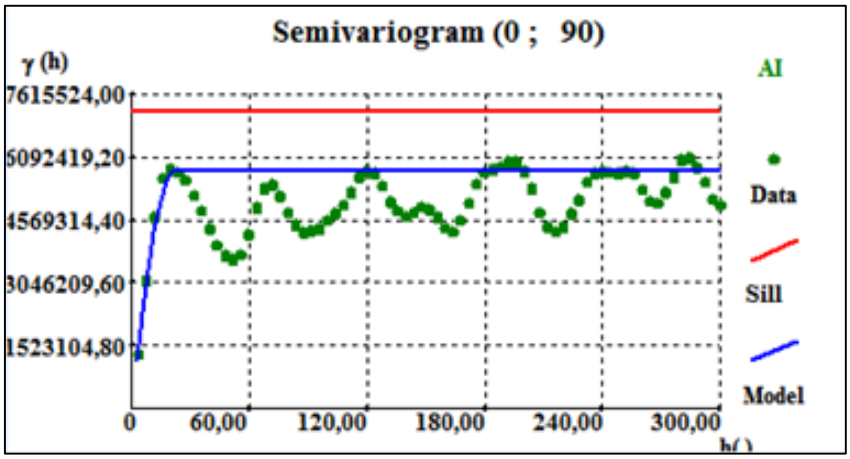

Figure 46. Vertical variogram (Green filled circles) and modeled variograms (blue line) calculated for the result of case 3.

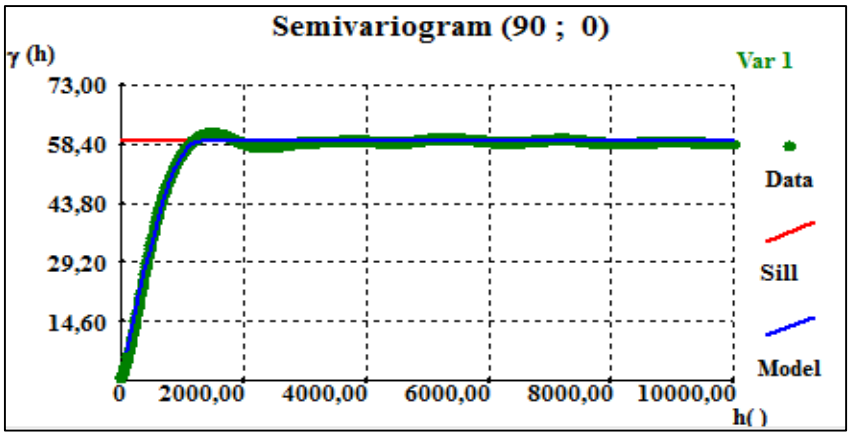

Figure 47. Horizontal variogram (Green filled circles) and modeled variograms (blue line) calculated for the result of case 3.

The best correlation section calculated in the inversion is in figure 48 and its statistics are show in figure 49, where is possible to observe that the high correlation is 0.99, the mean correlation is 0.93, being lower in noisy areas, where in the synthetic (figure 43) are observed problems in the definition of reflectors.

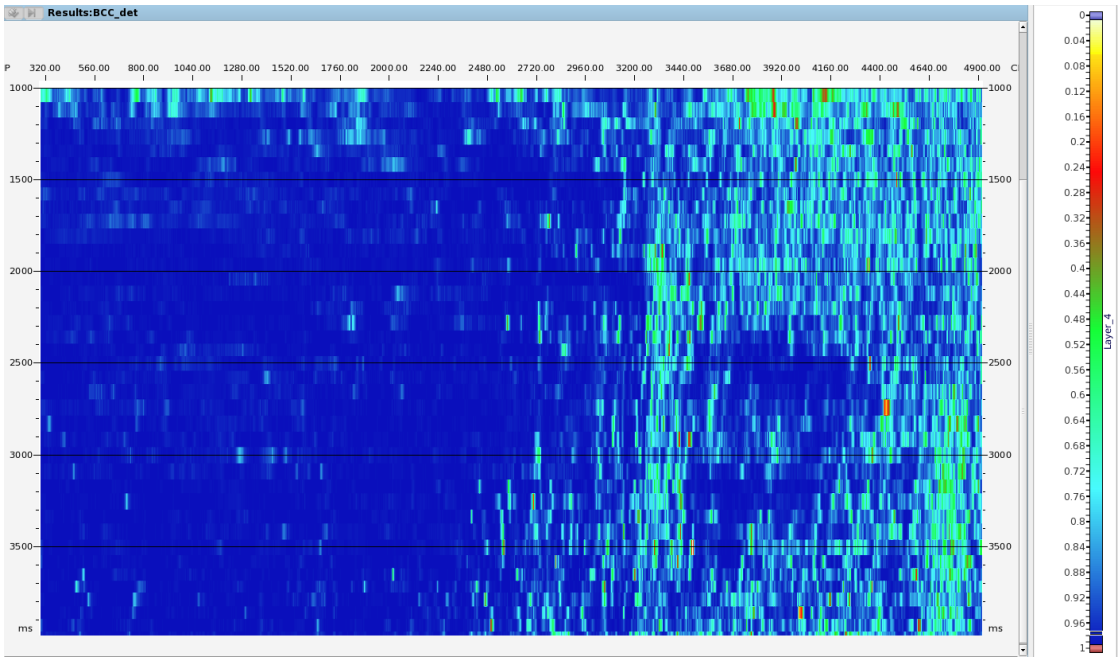

Figure 48. Best correlation section for case 3

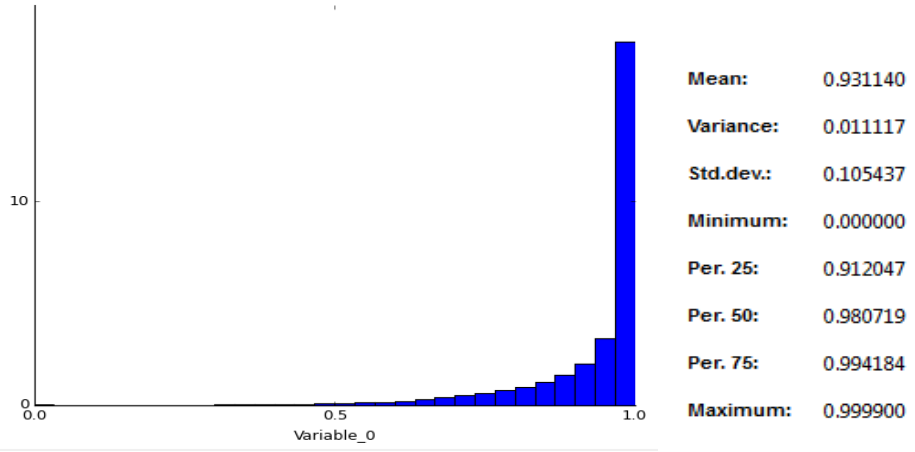

Figure 49. Histogram and statistics of the best correlation section for case 3

The mean for all the simulations of the last iteration was calculated and is in figure 48, where can be observed that in areas where the synthetic has a bad definition of the reflectors, this looks smoother than the best acoustic impedance section (figure 43). The histogram (figure 49) shows a minimum value equal to 5345 (m/s)*(g/cc), which is higher than the minimum value of the input model 5152 (m/s)*(g/cc) and a maximum value equal to 27294 (m/s)*(g/cc), which is slightly lower compared to the value of the input model 27331 (m/s)*(g/cc).

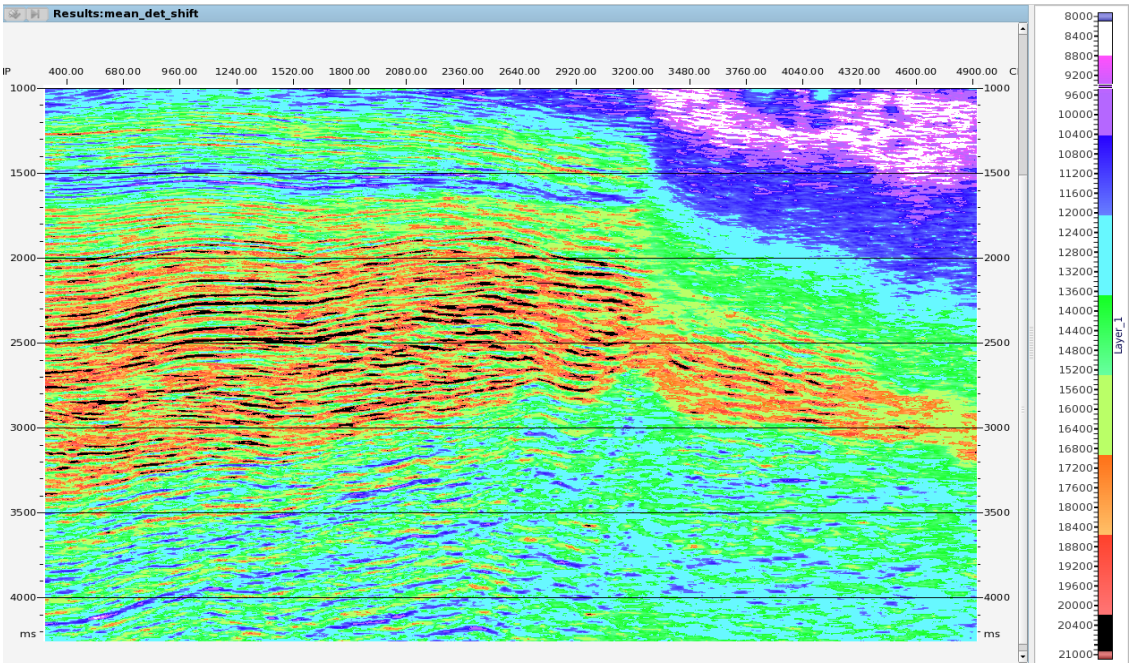

Figure 50. Mean calculated for case 3

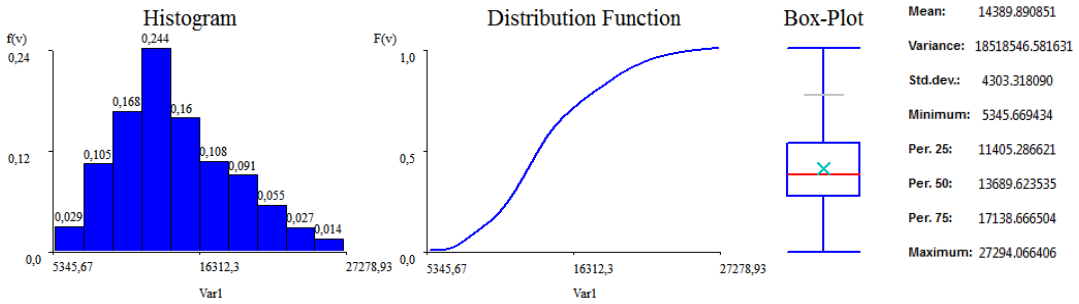

Figure 51.Histogram and statistics of the mean calculated for case 3.

Figure 52 represents the variance calculated taking into consideration the 32 simulation of the last iteration, which is high in areas where the seismic information has a low signal-noise ratio and the synthetic calculated during the inversion has a poor definition of the events. Also the variance is high in zones where the main structure has an important lateral change.

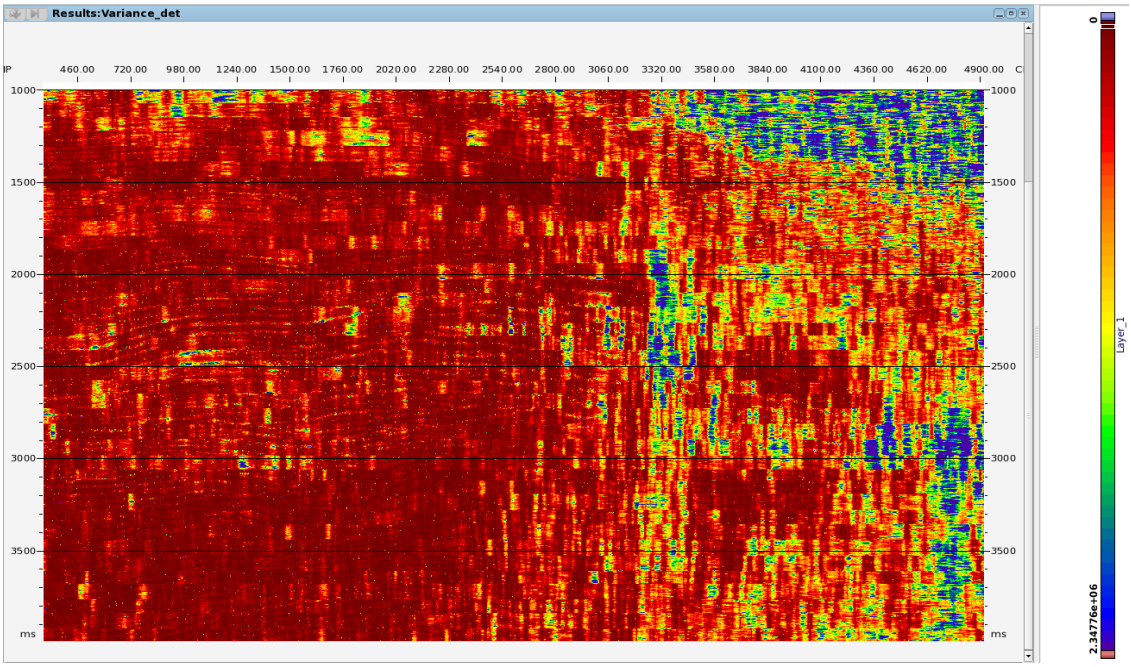

Figure 52. Variance calculated for 3.

6. CONCLUSIONS

The final results have shown that the Global Stochastic Inversion for acoustic impedance is a suitable technique to be apply in reservoirs in total absence of well data and makes possible an assessment of the uncertainty given by the calculation of the best correlation section and the variance of the simulations.

The new approach proposed in this study by integrating the result of a fast deterministic inversion as prior image of acoustic impedance in the Global Stochastic Inversion has shown a promising result and can be considered as a valid alternative to perform seismic inversion in under-sampled reservoirs.

The use of local models in the Global Stochastic Inversion shown that this approach is also a promising technique when the geological knowledge is sufficient.

The variance in all the cases studied gave high values in areas where the quality of the seismic data is reduced. In those areas lower values of correlation were obtained, which means that at the end of the inversion process those remain poorly matched.

The result of the model-based inversion reproduces the seismic data and also the noise in it. This could represent a problem when the data has poor quality, because create artifacts in the inverted section. Nevertheless, this methodology shown to be useful to generated pseudo-logs of acoustic impedance that reflect the vertical variability of the property.

Variograms for the best acoustic sections were performed, which revealed that the technique is reproducing the spatial continuity of the data. However, calculated values for the sill in all the cases were very different to the sill of the variograms calculated for the input data, which means that the level of variability of the property is not being reproduced, this is more evident for the vertical variograms.

In order to obtain a better image of best acoustic impedance in case 2, it is recommended to perform the flattening of the data to avoid the miscalculation in places where the structure generates important lateral changes in the value of the property.

It is also recommended to use the deterministic inversion to generate one pseudo-log in each trace in order to have a better estimation of the property in all the areas, this could help to have a better estimation due to the lateral variation of the property.

Combing a deterministic approach and a stochastic approach to perform the inversion of acoustic impedance shown to be a suitable solution for the limitation of quantity and quality of the data in under-sampled reservoirs.

REFERENCES

Aki, K., Richards, P.G. (1980). Quantitative Seismology, Theory and Methods, Vol. I and II, W.H. Freeman, San Francisco.

Azevedo, L., Nunes, R., Almeida J. Caeiro M., Correia, J. and Soares, A. (2012). Seismic Attributes for Constraining Geostatistical Seismic Inversion. Ninth International Geostatistics Congress.

Boschetti, F., Dentith, M.C, and List, R. D. (1996). Inversion of Seismic Refraction Data Using Genetic Algorithms. Geophysics, 61, 1715–1727. doi:10.1190/1.1444089.

Boore D. (2007). Some thoughts on relating density to velocity. Retrieved from: http://www.ce.memphis.edu/7137/PDFs/Boore/daves_notes_on_relating_density_to_velocity_v1.2.pdf .Accessed 18 January 2015.

Buland, A., and El Ouair, Y. (2006). Bayesian Time-Lapse Inversion. Geophysics, 71, R43–R48. doi:10.1190/1.2196874.

Buland, A., and More, H. (2003). Bayesian Linearized AVO Inversion. Geophysics, 68, 185–198.

Chopra and Castagna (2014). Investigation in Geophysics No. 16: AVO Satinder Chopra, John P. Castagna

Doyen, P. (2007). Seismic reservoir characterization: European Association of Geoscientists & Engineers

Francis A. (2005). Limitations of Deterministic and Advantages of Stochastic Seismic Inversion. Retrieved from: http://cseg.ca/technical/view/limitations-of-deterministic-and-advantages-of-stochastic-seismic-inversion. Accessed 21 January 2015.

Gardner, G.H.F., Gardner, L.W., and Gregory, A.R. (1974). Formation velocity and density – The diagnostic basics for stratigraphic traps. Geophysics, 39, 770-780.

Gavotti P. (2014). Model-based inversion of broadband seismic data. Degree of Master of Science. Department of Geoscience, University of Calgary.

Grana, D., and Della Rossa, E. (2010). “Probabilistic Petrophysical-Properties Estimation Integrating Statistical Rock Physics with Seismic Inversion.” Geophysics, 75, O21–O37. doi:10.1190/1.3386676.

Lindseth R. (1979). Synthetic sonic logs- A process for stratigraphic interpretation: Geophysics, 44, 3-26.

Mallick, Subhashis. (1995). Model Based Inversion of Amplitude Variations with Offset Data Using a Genetic Algorithm. Geophysics 60, 939–954. doi:10.1190/1.1443860.

Mallick, Subhashis. (1999). Some Practical Aspects of Prestack Waveform Inversion Using a Genetic Algorithm: An Example from the East Texas Woodbine Gas Sand. Geophysics 64, 326–336.

Russell B. (1988). Introduction to seismic inversion methods. Society of Exploration Geophysicist, Course Note Series, 02.

Russell, B., and D. (1991), Comparison of post-stack inversion methods: 61St Annual International Meeting, SEG, Expanded Abstracts, 10, 876-878.

Schlumberger Oil Field Glossary. Diagram of reflection and refraction. Retrieved from: http://www.glossary.oilfield.slb.com/en/Terms/r/reflection.aspx. Accessed on 27 December 2014.

Simm R. and Bacon M. (2014). Seismic Interpretation Handbook. Cambridge University Press.

Soares A. (2006). Geostatistics for Earth Sciences and Environment (2nd Ed.). IST Press, Lisboa.

Soares, A., Diet, J.D., and Guerreiro, L. (2007). Stochastic Inversion with a Global Perturbation Method. Petroleum Geostatistics, EAGE, Cascais, Portugal (September 2007), 10–14.

STRATA user guide. (2009). Hampson-Russell Assistant: STRATA Theory. Hampson Russell Software, a CGG Company.

Tarantola, A. (2005). Inverse Problem Theory. SIAM.

Usman S. (2013). Acoustic and Elastic Impedance Models of Gullfaks Field by Post-Stack Seismic Inversion. Bachelor Degree in Petroleum Geosciences.Department of Petroleum Engineering and Applied Geophysics, Norwegian University of Science and Technology

Yilmaz, O. (1987). Seismic Data Processing. Society of Exploration Geophysicis

APPENDIX

In this section is shown and described the processing sequence applied to the data seismic data (figure 53). This sequence was performed from field data until pre-stack time migration, using ECHOS, which is a commercial software developed by Paradigm.

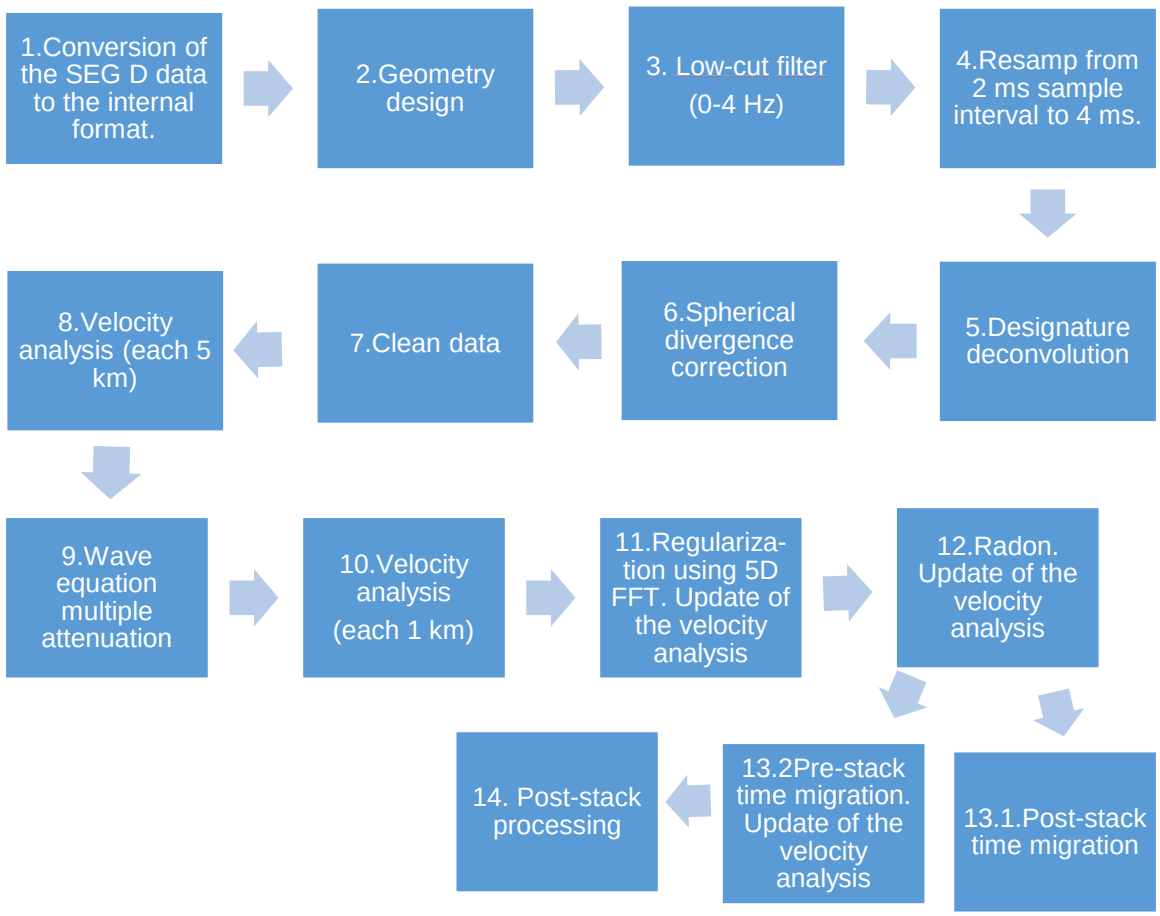

Figure 53. Seismic processing sequence

1. Conversion of the SEG-D to the internal format

In this initial stage is performed the conversion of the field to the internal format used in Echos. The input data was in a SEG-D format ordered by field file ID.

2. Geometry design

To perform the seismic processing a fake geometry was designed using the module MARINE. This module is a macro that generates all the geometry for a conventional marine line and considers that the spaces between stations and CDP's are constant and therefore the fold is uniform across the lines. It is important to mention that the acquisition parameters were considered during the design.

3. Low cut filter

A low cut filter to attenuate the swell noise were applied. In this case the filter had frequencies between 0 and 4 Hz.

4. Resampling

In order to decrease the running time of the processes the data were resampled from 2 ms to 4 ms. Prior to resampling an anti-alias filter was applied.

5. Designature deconvolution

In this case the seismic source signature was not available. To perform the designature deconvolution a minimum phase filter was designed then applied to the data. The software has a tool called Wavelet Utility, which makes possible the design of matching filters using a trace extracted from seismic.

6. Spherical Divergence correction

When the acoustic wave travels from the source through the subsurface its energy is spread out in all directions like a sphere and the area increases in width as time increase. This wavefront spreading results in a loss of energy in the seismic signal that causes a decrease in the amplitude with time, known as spherical divergence. A correction is used to compensate the effect in the amplitude and consist in the application of a gain function.

7. Clean Data

To attenuate the noise in the data a sequence was perfomed. The steps flowed in the sequence arepresented in the next sub-sections.

7.1 Band limited noise suppression (Supress).

It is used to perform time-variant band-limited noise suppression, such as ground-roll, swell noise, air blast, etc. This module decomposes the seismic trace into noise and signal components by filtering the trace for a specific frequency band (In this case from **0 to 18 Hz**). Finally, the noise component is then subtracted from the input trace to yield the signal component of the data.

7.2 Amplitude scaling for noise attenuation (AMPSCAL).

This process is used to perform noise attenuation (noise bursts, cable slashes, air blasts, etc.) through amplitude scaling. The data is analyzed across small overlapping spatial and temporal windows by comparing the window amplitude with the amplitude of corresponding window on neighboring traces in the dataset. Windows with anomalously high amplitudes are scaled down.

7.3 Low Frequency Array Filtering (LFAF).

Attenuates the noise originated by surface waves using Low-Frequency Array Forming. Given the surface velocity and a low frequency band, the algorithm first transforms the data from the time-space domain to the frequency-space domain. Next each frequency component is convolved with a boxcar function, which is the appropriate calculated array to cancel the shot generated noise train with the specified velocity. In this case frequencies between **0 and 20 Hz** were attenuated.

Figure 54 shows the comparison for one shot between the data before and after the application of the cleaning processing sequence. The output show is visible cleaner and the amplitude is more balance than in the input shot.

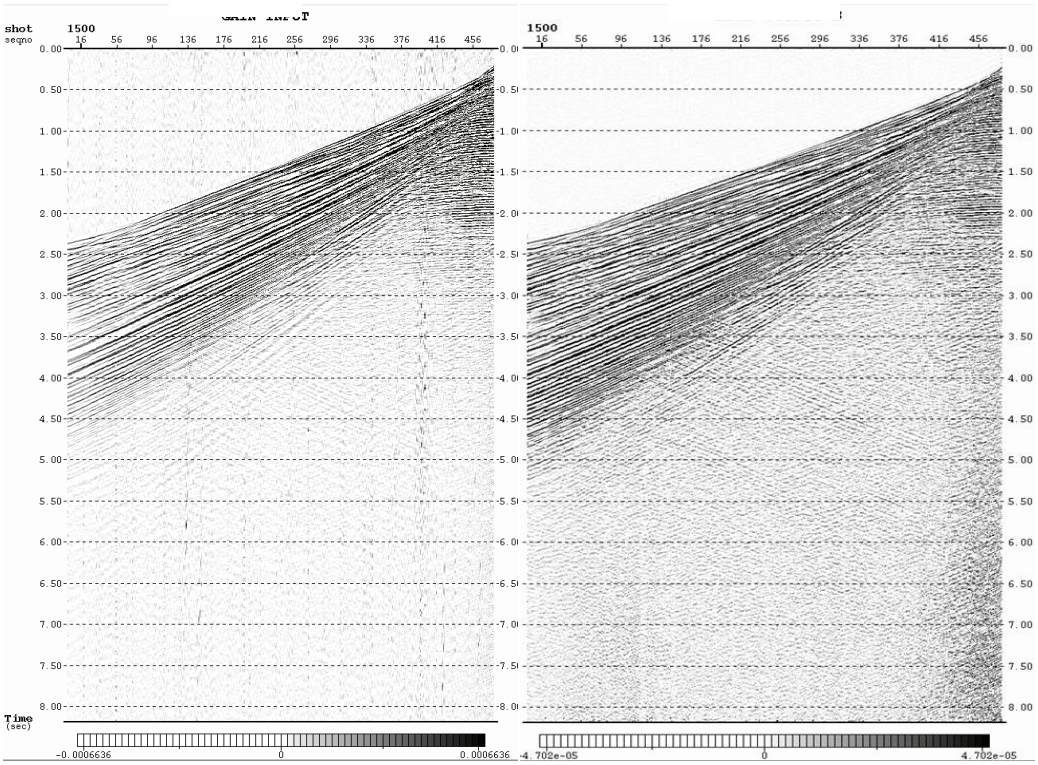

Figure 54. Shot before and after the cleaning processing sequence application

8. Velocity Analysis each 5 km.

A first velocity analysis each 5 km were perform after the cleaning process. In order to reduce the stretching of the data in large offsets a mute was picked and applied to the gathers. It is important to mention that was picked only one mute for all the CDP gathers in each line. The velocity analysis is performed using the VELDEF module, which makes possible to perform an interactive correction using the semblance, the normal moveout corrected gathers and mini-stacks are generated for a set of velocity functions that are referenced to a central velocity function.

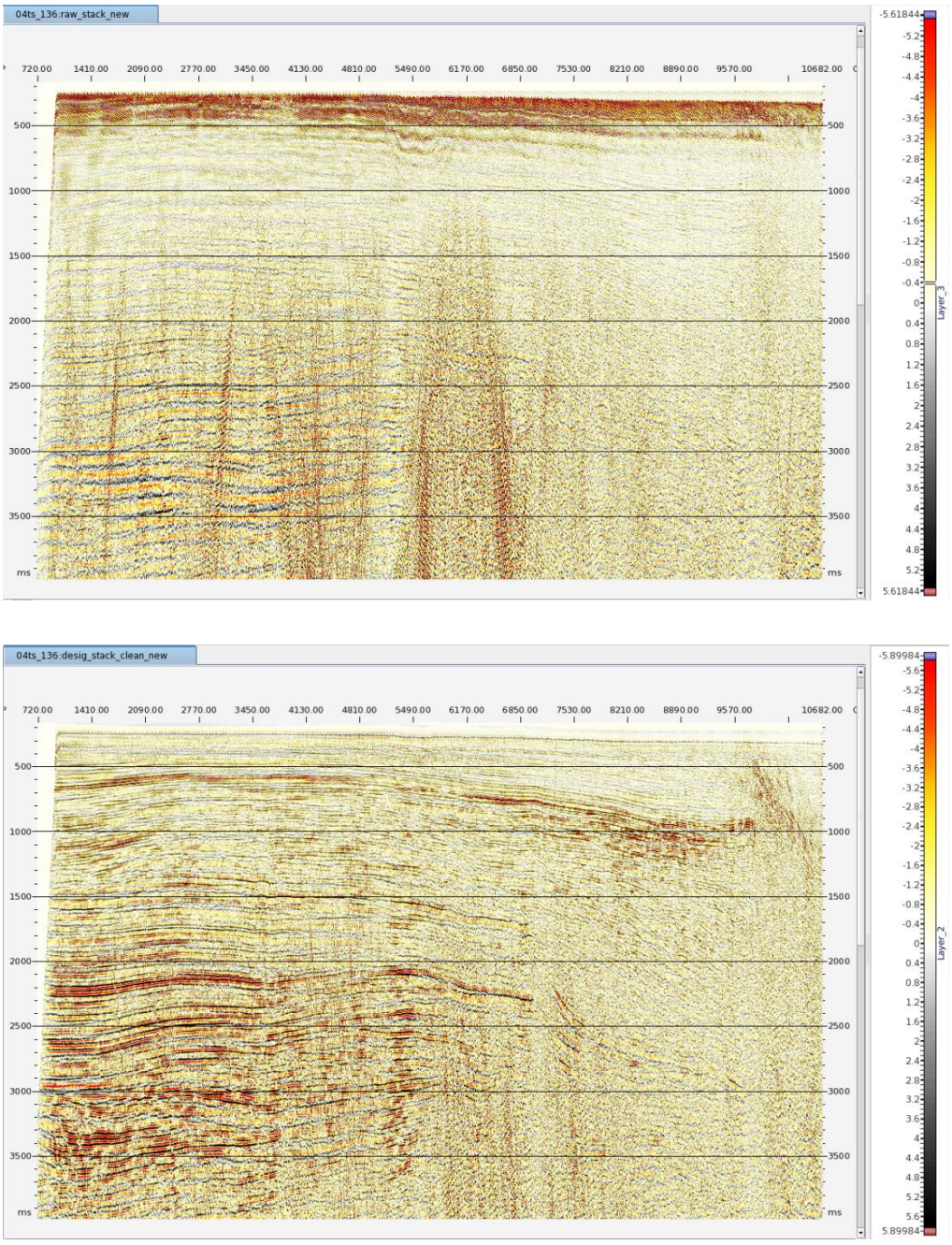

Figure 55. Stacks before (top) and after the cleaning processing (bottom) application in shot domain.

After the velocity analysis stacks of the data before and after the cleaning processing were performed. These stacks are shown in figure 55, where it is possible to observe that the cleaning processing helping to attenuate the low frequency noise in the data and therefore allowing the identification of seismic events.

9. Wave equation multiple attenuation (WEMA)

This module is a wave equation based multiple attenuation that performs multiple modeling and adaptive subtraction in shot domain. This module needs as input the water depth bellow the receiver location, which in this case was not available, for that reason was necessary to use a constant value of 150 meters obtained in the acquisition reports. The absent of real values of water depth for each receiver could cause problems in the performance of the module and for that reason was necessary to implement additional algorithms to perform multiple attenuation.

10. Velocity Analysis each 1 km.

A second velocity analysis each 1 km was performed after the WEMA. The density in the analysis is incremented to have a better definition and more continuity in the seismic reflectors. Next figure shows the velocity analysis performed for one CDP.

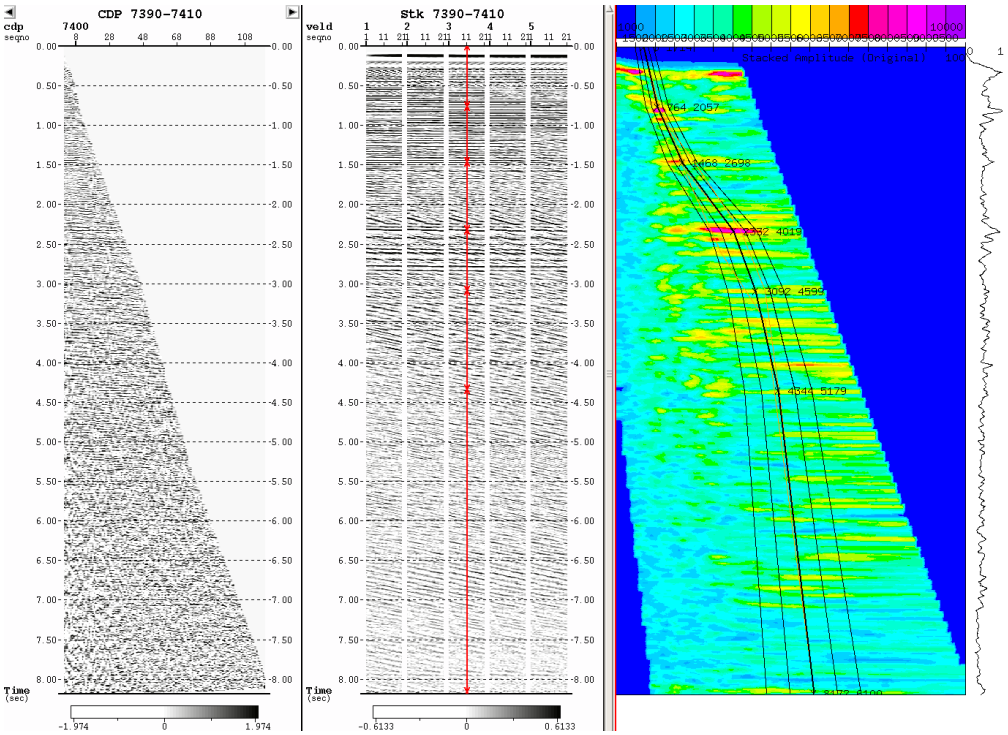

Figure 56. Velocity analysis each 1 km performed after WEMA.

11. Regularization using (up to) 5D FFT (INTRP5D).

In figure 57 it is possible to observe that the CDP gathers have a strong presence of noise, that made difficult the velocity analysis after the application of WEMA, for that reason was necessary to apply a regularization of the data in order to attenuate random noise in the gathers. After the INTRP5D module application an update in the velocity field was performed.

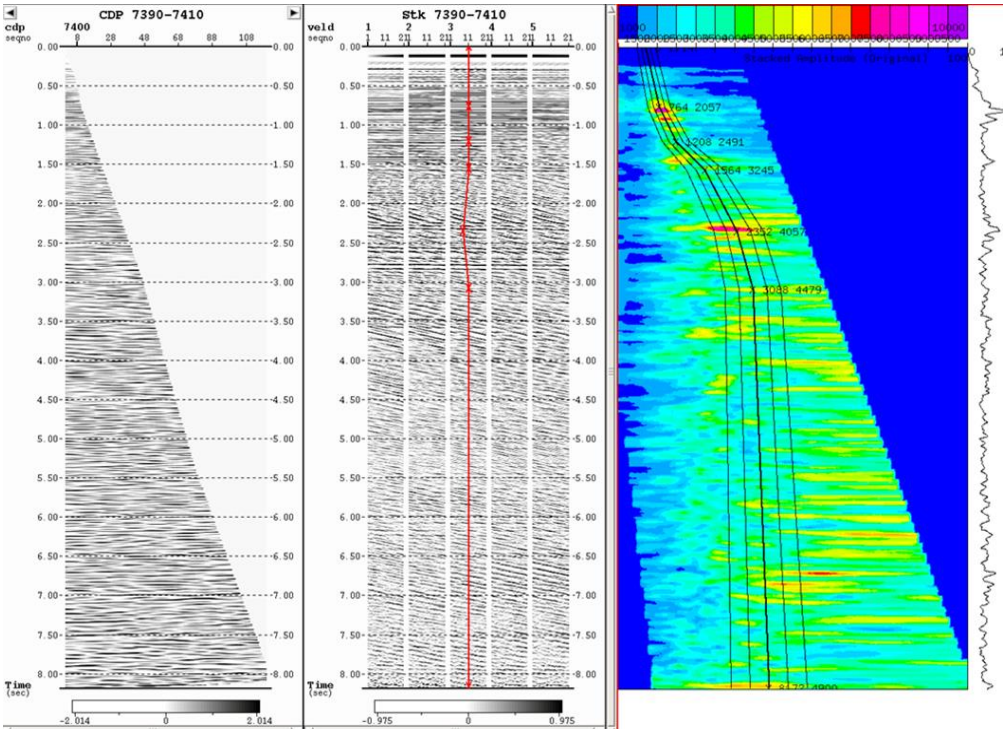

Figure 57. Velocity analysis each 1 km performed after INTRP5D.

12. Parabolic Radon Transform (RADNPAR)

It is applied to perform a parabolic Radon transform on input gathers that has been corrected for normal moveout. This module transforms the data from t-x domain into tau-p domain. In the tau-p domain is specified the zone where the primary energy is and then an inverse transform on the remaining multiple energy back to the t-x domain is performed. Finally, the result is subtracted from the original data remaining only the primary energy. After the application of the RADNPAR it is performed a new update in the velocity field.

13. Post-stack time migration

A Kirchhoff Post-stack time migration was performed. In Echos different types of Kirchhoff Post-stack time migration are available, depending on how the travel times are calculated. In this case the Hyperbolic travel time approximation was used, which performs the travel time calculation by curved

fitting 2nd (hyperbolic) or 4th (quartic). The travel time of a ray from the shot to the sub-surface CRP location (and back to the receiver) is calculated by straight ray approximation. The inputs for the migration were the stack generated after the application of RANDPAR in gathers and the smoothed version of the RMS velocity section obtained in from the last velocity analysis.

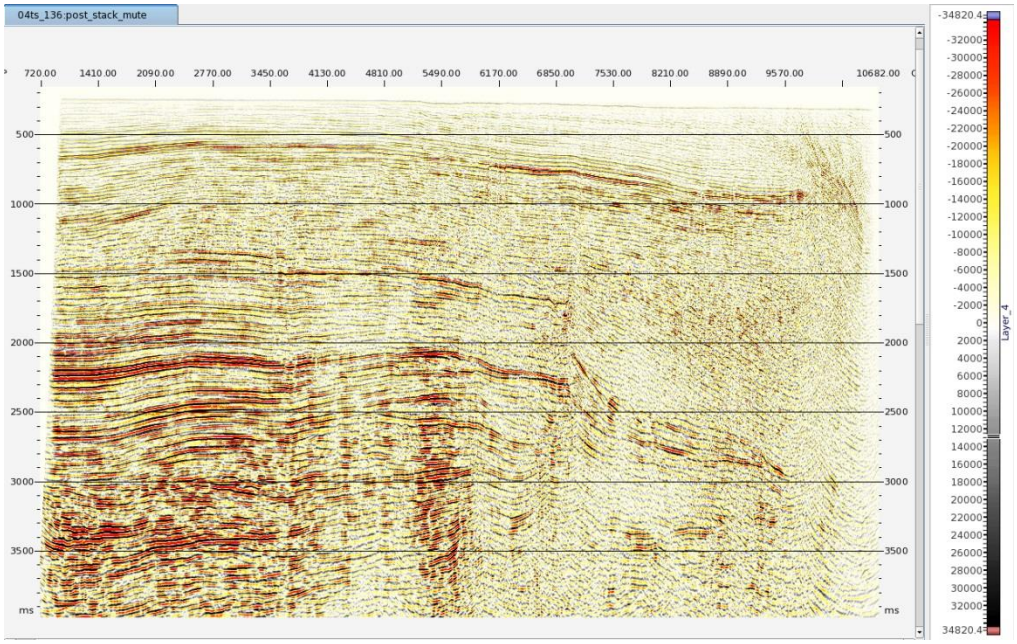

Figure 58. Post-stack time migration

14. Pre-stack time migration

A pre-stack time Kirchhoff migration was performed. The algorithm use a curved rays travel time approximation, in which the travel time is calculated by isotropic 1D ray tracing. This method traces the ray path on a 1D interval velocity model and are taken into account curved rays for the migration. The input for the migration were the gathers without normal moveout correction and the smoothed version of the interval velocity section.

15. Pre- stack time migration with post-processing

After the Pre-stack time migration and stack a post-processing sequence was applied with the goal of suppress the noise, balance the amplitude, give more continuity to the reflectors and enhanced some reflectors in the target area. Figure 59 represents the processing flow used in this stage.

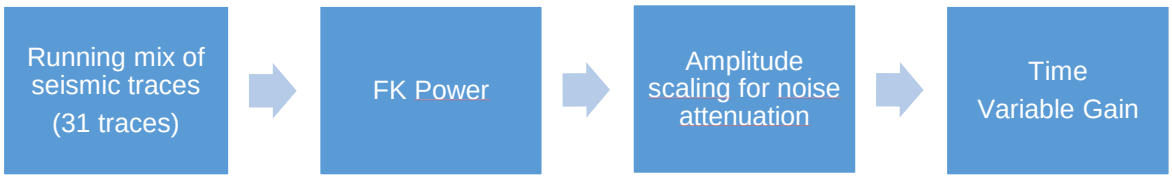

Figure 59. Post-processing flow

15.1 Running mix of seismic traces. In order to eliminate the noise in the stack a weighted trace mixing of 31 traces was applied.

15.2 FK Power. It is used to enhance the signal in a window of seismic data. The window of data in transform into the F-K domain. Is necessary to introduce three parameters:

1) POW. Specifies the power to which each F-K sample should be raised. In this case was POW=1.25.

2) TLEN. Specifies the time window length in milliseconds. In this case TLEN= 200 ms.

3) XLEN. Specifies the spatial window in number of traces. In this case XLEN=1000 traces.

15.3 Amplitude scaling for noise attenuation. This module analyses the data overlapping spatial and temporal windows by comparing the window amplitude with the amplitude of corresponding window on neighboring traces. Then windows with anomalously high amplitudes are scaled down. In this case the amplitude was scaling each 200 traces and in temporal windows of 200ms.

15.4 Time variable gain. Applied to balance the seismic amplitude in the stack.

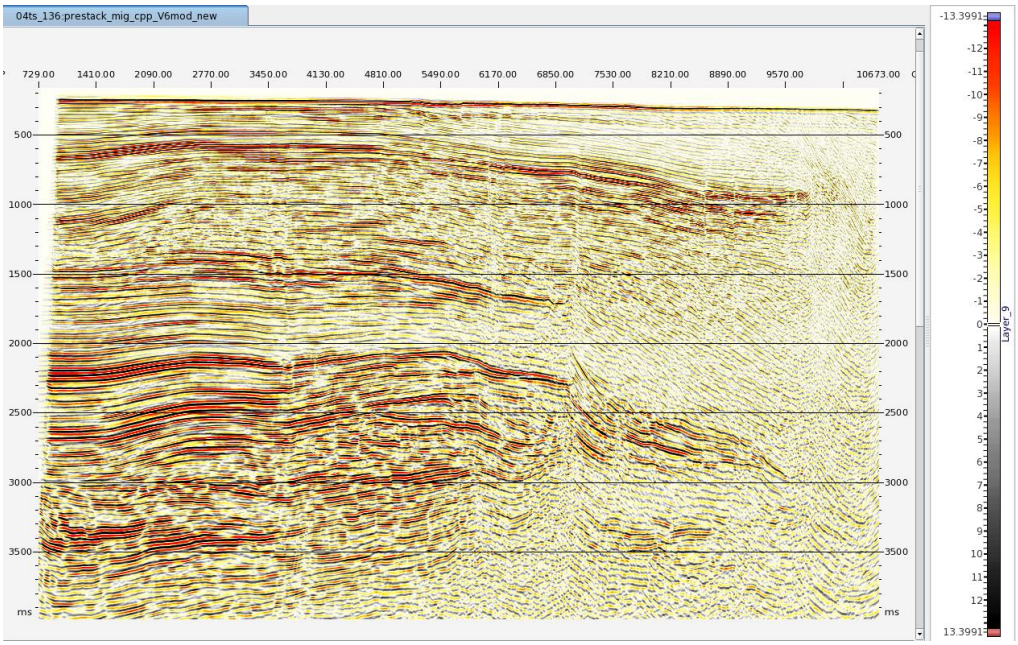

Figure 60. Stack of pre-stack time migration with post-processing

It is important to mention that after the Post-stack processing, a bulk shift and the real geometry were applied to the data. The bulk shift is related with the instrument delay correction (-150 ms) and the gun

and cable depths compensation (8ms). These values were obtained from the report of the previous processing.

The final output obtained after these corrections represents the input seismic data of this project.